Article

iPS-cell-derived microglia promote brain organoid maturation via cholesterol transfer

https://doi.org/10.1038/s41586-023-06713-1

Received: 18 March 2021

Accepted: 4 October 2023

Published online: 1 November 2023

Check for updates

Dong Shin Park[1,2,23], Tatsuya Kozaki[1,23], Satish Kumar Tiwari[1], Marco Moreira[3], Ahad Khalilnezhad[1,2], Federico Torta[4,5], Nicolas Olivié[6], Chung Hwee Thiam[2], Oniko Liani[1], Aymeric Silvin[1,3], Wint Wint Phoo[7], Liang Gao[4,5], Alexander Triebl[4,5], Wai Kin Tham[5], Leticia Gonçalves[3], Wan Ting Kong[1,3], Sethi Raman[1], Xiao Meng Zhang[1], Garett Dunsmore[3], Charles Antoine Dutertre[1,3], Salanne Lee[1], Jia Min Ong[1], Akhila Balachander[1], Shabnam Khalilnezhad[1,8], Josephine Lum[1], Kaibo Duan[1], Ze Ming Lim[1], Leonard Tan[1], Ivy Low[1], Kagistia Hana Utami[9], Xin Yi Yeo[10], Sylvaine Di Tommaso[11], Jean-William Dupuy[12], Balazs Varga[13], Ragnhildur Thora Karadottir[13], Mufeeda Changaramvally Madathummal[14], Isabelle Bonne[2], Benoit Malleret[1,2,14], Zainab Yasin Binte[1], Ngan Wei Da[1], Yingrou Tan[1], Wei Jie Wong[15], Jinqiu Zhang[9], Jinmiao Chen[1], Radoslaw M. Sobota[7], Shanshan W. Howland[1], Lai Guan Ng[1,2,16], Frédéric Saltel[11], David Castel[17], Jacques Grill[17], Veronique Minard[3], Salvatore Albani[8], Jerry K. Y. Chan[18], Morgane Sonia Thion[6], Sang Yong Jung[10,19], Markus R. Wenk[4,5], Mahmoud A. Pouladi[9,20,21], Claudia Pasqualini[3], Veronique Angeli[2], Olivier N. F. Cexus[5,10,22] & Florent Ginhoux[1,2,3,8,15] ✉

Microglia are specialized brain-resident macrophages that arise from primitive macrophages colonizing the embryonic brain[1]. Microglia contribute to multiple aspects of brain development, but their precise roles in the early human brain remain poorly understood owing to limited access to relevant tissues[2–6]. The generation of brain organoids from human induced pluripotent stem cells recapitulates some key features of human embryonic brain development[7–10]. However, current approaches do not incorporate microglia or address their role in organoid maturation[11–21]. Here we generated microglia-sufficient brain organoids by coculturing brain organoids with primitive-like macrophages generated from the same human induced pluripotent stem cells (iMac)[22]. In organoid cocultures, iMac differentiated into cells with microglia-like phenotypes and functions (iMicro) and modulated neuronal progenitor cell (NPC) differentiation, limiting NPC proliferation and promoting axonogenesis. Mechanistically, iMicro contained high levels of PLIN2$^+$ lipid droplets that exported cholesterol and its esters, which were taken up by NPCs in the organoids. We also detected PLIN2$^+$ lipid droplet-loaded microglia in mouse and human embryonic brains. Overall, our approach substantially advances current human brain organoid approaches by incorporating microglial cells, as illustrated by the discovery of a key pathway of lipid-mediated crosstalk between microglia and NPCs that leads to improved neurogenesis.

In the early stages of embryonic development, primitive macrophages colonize the brain and differentiate into microglia[1]. Studies in animal models show that microglia play important roles during brain development, including regulating the number and differentiation of neuronal progenitor cells (NPCs) through neuronal death[3], phagocytosis[2,4] and release of pro-inflammatory cytokines[5]. Microglia also participate in shaping prenatal forebrain circuits, controlling the outgrowth of dopaminergic axons in the forebrain and the laminar positioning of subsets of neocortical interneurons[6]. However, their roles in human brain development are largely unknown because access to human embryonic brains for research is limited.

Recent advances in stem cell technologies have allowed the generation of human induced pluripotent stem (iPS) cell-derived three-dimensional (3D) brain organoids that mimic embryonic brains[7–10] and develop neuroepithelial rosettes that resemble the developing cerebral cortex and contain intermediate progenitor cells and different subtypes of cortical neurons[7–10]. Despite transcriptomic studies further showing that the neuronal cell types generated in organoids are similar to their counterparts in the human embryonic brain[10–12], these organoids are devoid of non-neuronal cell types, such as endothelial cells and microglia, that are essential for correct brain development and maturation[13,14].

Exploiting our protocol for producing human iPS cell-derived primitive macrophages (iMac) that can differentiate into microglia-like cells (iMicro) in the presence of neuronal cells[15], we generated microglia-sufficient human iPS cell-derived brain organoids. iMac

A list of affiliations appears at the end of the paper.

penetrated into the organoids, displayed activated morphology, demonstrated key microglial functions and expressed microglia-associated genes and regulons. Their addition led to an atrophy of neural rosettes with reduced proliferation of NPCs and enhanced axonogenesis and synaptogenesis, supported by an increase in electrophysiological activity. This was driven by iMicro rich in PLIN2$^+$ lipid droplets orchestrating cholesterol efflux via ABCA1, its esterification, and increased levels in organoids. NPCs acquiring this exogenous cholesterol show marked metabolic reprogramming accompanying their differentiation into neuronal cells. These PLIN2$^+$ lipid droplet-loaded microglia were detected in mouse and human embryonic brains, consistent with parallel processes occurring in vivo. Overall, we present a method for the generation of more accurate and relevant microglia-sufficient brain organoids, adding a valuable tool for understanding the role of microglia in human brain development and enabling us to unravel a key mechanism of communication between embryonic microglia and NPCs.

iMac differentiate into microglia-like cells

Microglia are detected in the developing human brain as early as 4.5 weeks after conception[16,17]. To generate microglia-containing organoids mimicking the embryonic brain, we first differentiated cerebral organoids[7,8] and iMac[18] from the same human iPS cells for 26 days, at which point organoid development mirrors major aspects of human brain development in vivo[22]. We then mimicked the influx of a first wave of microglial progenitors[1] by introducing iMac into organoid cultures at day 26 (herein referred as day 0; Fig. 1a and Extended Data Fig. 1a). We verified that the change of medium did not affect iMac phenotype at day 1 (Extended Data Fig. 1b) and day 15 (ref. 23) (Extended Data Fig. 1c). At day 18 of coculture, IBA1$^+$ iMac were on the surface of each organoid as individual cells and clusters (Fig. 1b and Extended Data Fig. 1d). iMac also penetrated the organoids while displaying an amoeboid morphology typical of embryonic microglia[2,16] (Fig. 1c, Extended Data Fig. 1d,e and Supplementary Video. 1). Some iMac also showed signs of proliferation (Ki67; Extended Data Fig. 1f).

Phenotypically[24], iMac within organoids expressed significantly higher levels of *P2RY12*, *CX3CR1* and *SALL1*, but not *TMEM119*, in day 15 and day 30 cocultures than iMac alone (Fig. 1d). This was not observed in iMac cocultured in two dimensions with cortical neurons for 14 days (ref. 22), thus suggesting that the 3D coculture favoured the expression of typical markers of microglia at the transcriptomic level (Extended Data Fig. 2a). Accordingly, CD45$^+$CD14$^+$CD163$^+$CD11b$^+$ iMac (Extended Data Fig. 2b) in 15-day cocultures expressed higher levels of P2RY12 and CX3CR1 protein, but not TMEM119 protein (Fig. 1e and Extended Data Fig. 1g). With various reports questioning the reliability of TMEM119 in solely describing all microglial cells[25,26] and its typical expression in postnatal microglia[27], this indicated that our brain organoids were successfully supporting the development of iMac bearing an embryonic microglial phenotype, lacking TMEM119. We then investigated whether iMac acquired typical in vivo microglial functions within brain organoids. iMac rapidly extended their dendrites towards sites of laser-induced neuronal 'injury'[28] (Extended Data Fig. 1h and Supplementary Video 2) and, actively moving over the organoid surface, some iMac phagocytosed pathogenic amyloid-β peptides associated with Alzheimer's disease[29] (Extended Data Fig. 1i and Supplementary Video 3).

Next, to gain insight into the transcriptomic changes in iMac induced by coculture with organoids, we performed single-cell RNA sequencing (scRNA-seq) of iMac cultured alone, organoids alone and organoids cocultured for 18 days (Extended Data Fig. 2c), and analysed data from 9,780 cells (Extended Data Fig. 2d,e,f) using Seurat-V3 (ref. 30). We then performed principal component analysis of normalized read counts followed by dimensionality reduction using *t*-distributed stochastic neighbour embedding (*t*-SNE)[30]. Using the expression of marker genes, we identified neurons (*STMN2*, *MYT1L*, *DCX*, *NRXN1*, *MAP2*, *SNAP25*, *TUBB3*), NPCs (*CXCR4*, *NES*, *PAX6*, *SOX2*, *GLI3*, *HES1*, *VIM*, *ID2*), mesenchymal cells (*DCN*, *LUM*, *COL1A2*, *COL5A1*) and macrophages/microglia (*PTPRC*, *AIF1*, *ITGAM*, *CD68*) (Fig. 1f,g and Extended Data Fig. 2g,h,i). We then performed a differentially expressed gene (DEG) analysis between iMac from organoid cocultures and iMac alone (Extended Data Fig. 3a,b and Supplementary Table 1) and subjected our data to single-cell regulatory network inference and clustering (SCENIC) analysis to map their gene regulatory networks[31] in order to identify differential activity of regulons (units of single transcription factors and their putative target genes). iMac from coculture organoids had upregulated the activity of *IRF1,2,7,8* as well as *CEBP*, *MAF*, *EGR* and *AP-1* regulons (Fig. 1h,i, Extended Data Fig. 3c and Supplementary Table 2), involved in the acquisition of microglial identity during brain development[24]. These results show that iMac in organoids differentiate into microglia-like cells (hereafter called iMicro) (Extended Data Fig. 1a).

We then tested whether iMicro were improving neuronal function by addressing the electrophysiological maturation of neurons using patch-clamp characterization analysis[32]. The presence of iMicro increased the frequency of maximum action potential firing (Fig. 1j) and of second and third action potentials (Fig. 1k). The quantification of action potential firing patterns also showed that iMicro improved action potential firing patterns to a majority of immature, single mature and mature action potential train firing patterns (Fig. 1l and Supplementary Table 3). Neurons displayed significantly lower action potential threshold and resting membrane potential in coculture organoids (Fig. 1m). However, at this early time point of coculture (day 14), no functional synaptic properties such as capacitance (Extended Data Fig. 4a), spontaneous postsynaptic currents determined by their amplitude and frequency (Extended Data Fig. 4b,c,d), or spontaneous postsynaptic current kinetics characterized by their associated rate time and decay time (tau) were changed in the presence of iMicro (Extended Data Fig. 4e,f). These results nevertheless highlighted that iMicro promoted functional maturation of neurons in cocultured organoids.

Altogether, iMac in organoids (iMicro) are able to detect and respond to a brain-like environment similarly to in vivo microglia, while promoting electrophysiological maturation of neurons, thus suggesting that iMicro support neurogenesis.

iMicro promote the maturation of neuronal cells

Microglia have pivotal roles in embryonic brain development by regulating the number and differentiation of NPCs[2–5]. While organoids generated from the KYOU1, XCL-1, HD33i and IMR-90 iPS cell clones showed continuous growth without iMicro, their growth was significantly reduced and organoids became smoother and rounder as early as 12 days after coculture (Fig. 2a, Extended Data Fig. 5a–d and Supplementary Videos 4 and 5). Absent in organoids generated from the KYOU1, HD33i and IMR-90 iPS cell clones (Fig. 1 and Extended Data Fig. 5d), innate microglia (innMicro) developed in organoids generated from CTRL, CAU, PCi-ASI and, to a much lesser extent, XCL-1 iPS cell clones[33,34] (Extended Data Fig. 5e). The development of innMicro using these iPS cells was organoid dependent, driven by the presence of colony-stimulating factor 1 (CSF-1) in the culture medium and linked to a reduction in size of the organoids compared to their counterparts devoid of innMicro (Extended Data Fig. 5e–g) in line with CSF-1 dependence of microglia[35,36]. We further confirmed the reduction in the size of organoids generated from iPS cell lines made from four paediatric patients with brain cancer (Extended Data Fig. 5h and Supplementary Fig. 2). Altogether, this repeatedly (Supplementary Table 4) suggested that the presence of either iMicro or innMicro led to the reduction in size of brain organoids.

Assessing the cellular composition of the organoid cultures[37], we observed that alongside a reduction in the total number of cells, the absolute and relative numbers of NPCs were significantly lower in the presence of iMicro (Fig. 2b). We then used our scRNA-seq to identify

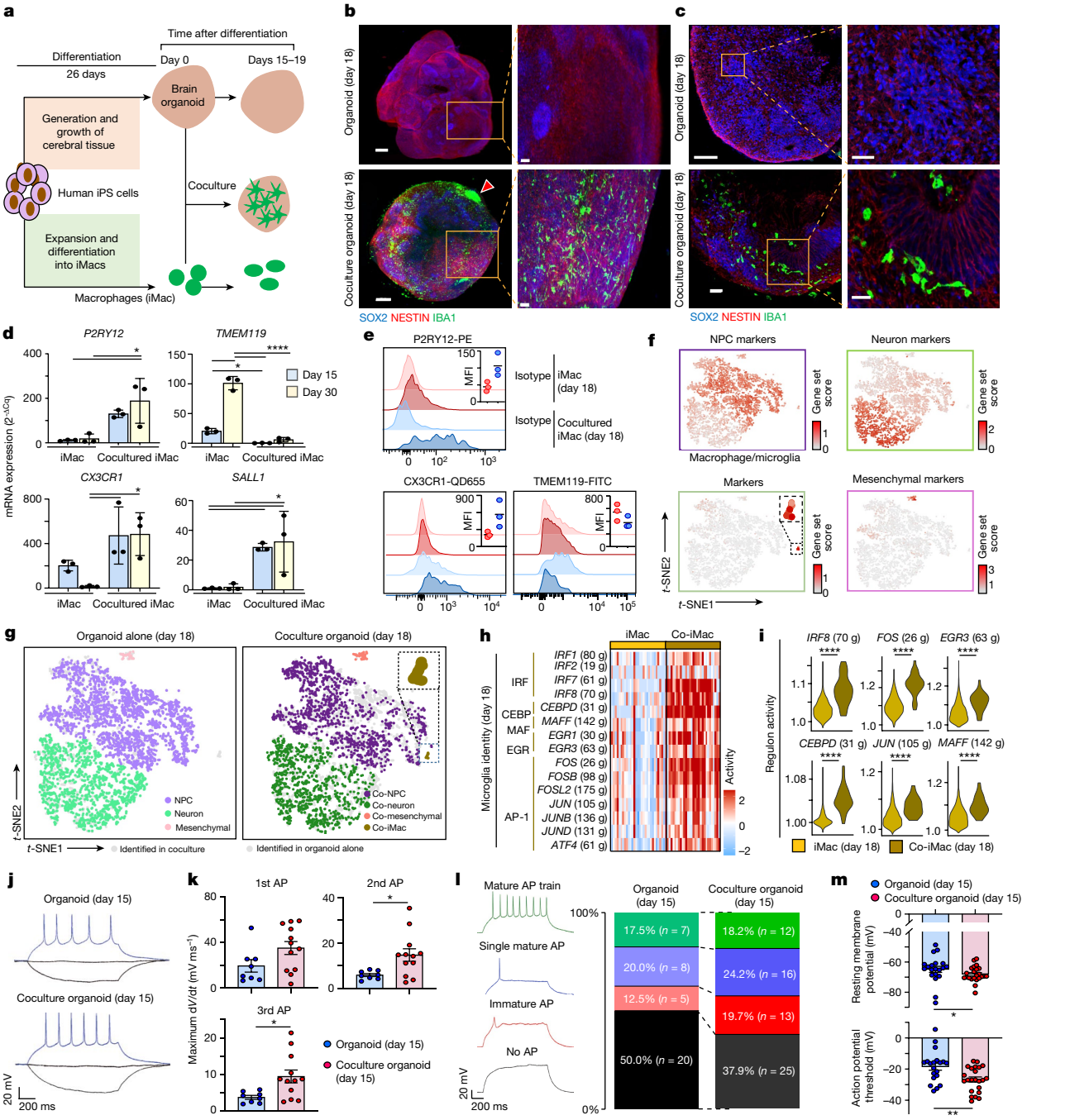

Fig. 1 | iMac become microglia-like cells in brain organoids. a, Generation of microglia-sufficient brain organoids resulting from coculture (constitute day 0) of iMac and brain organoids obtained 26 days after initial iPS cell culture. Cocultured organoids are analysed from 14 days after day 0. **b**, 3D images of brain organoids cocultured with or without iMac. Arrowhead indicates iMac cluster on organoid. Representative of $n = 3$. **c**, Sectioning and staining of day 18 organoids cocultured with or without iMac. Representative of $n = 4$. **d**, Expression of microglia-specific markers in iMac alone ($n = 3$) or cocultured with brain organoids ($n = 3$) by RT-qPCR (days 15 and 30). **e**, Expression of microglia-specific markers in day 18 iMac ($n = 3$) and iMac cocultured with organoids ($n = 3$) for 18 days. **f**,**g**, *t*-SNE plots on concatenated representations showing the gene set score for canonical markers used to define neurons, NPCs, iMac and mesenchymal cells in day 18 organoid and coculture organoids (**f**) and the projection of these different cell types, with cocultured iMac magnified in the right panel (**g**). **h**, Heatmap showing the expression levels of regulons involved in the acquisition of microglia identity in iMac and cocultured iMac (co-iMac) (**h**; g, genes) and violin plots comparing the expression levels of regulons involved in the acquisition of microglia identity between iMac and co-iMac (**i**). **j**, Representative voltage responses from whole-cell patch-clamp recordings at −50 pA, 0 pA and maximum action potential firing (bottom to top). **k**, Analysis of the first, second and third action potentials observed during maximum action potential firing of organoid ($n = 8$) and coculture ($n = 12$). **l**, Distribution of action potential firing patterns for neurons from control ($n = 40$) and coculture ($n = 66$) organoids (left panel, example traces). **m**, Intrinsic properties of neurons from each organoid ($n = 20$) and coculture organoids ($n = 23$). Statistical analysis, one-way ANOVA (**d**), Mann–Whitney test (**i**,**k**,**m**). Error bars, mean ± s.e.m. Scale bars, 300 µm (**b**), 100 µm (**b** (boxed area), **c**) and 20 µm (**c**, boxed area). $^*P \leq 0.05$; $^{**}P \leq 0.01$; $^{***}P \leq 0.001$; $^{****}P \leq 0.0001$. Asterisks above horizontal bars apply to all bars beneath them. More detailed legends for Figs. 1–4 are available in the Supplementary Information.

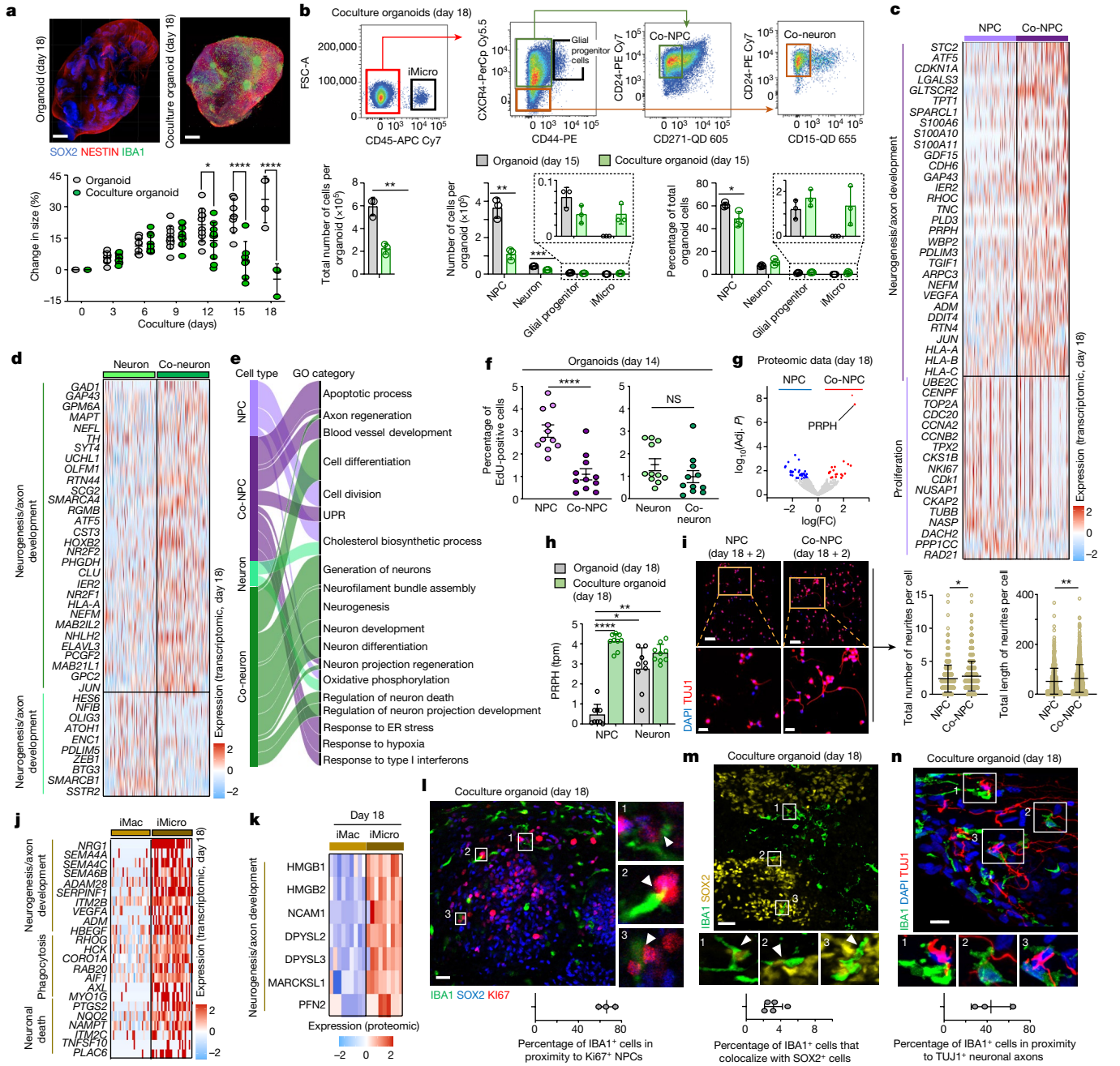

Fig. 2 | iMicro promote the maturation of neuronal cells in organoids. **a**, Top, 3D images of 18-day brain organoids and coculture organoids. Bottom, evolution of organoid sizes over time. (Each culture: $n = 10$ (day 0–10), $n = 7$ (day 12), $n = 3$ (day 18)). **b**, Top, gating strategy to define iMicro, NPCs, neurons and glial progenitor cells in cocultured organoids (day 18). Bottom, number and proportion of each cell type (day 15, $n = 3$). **c**,**d**, Heatmaps of the genes involved in neurogenesis (and axon development) and proliferation preponderant in co-NPCs and NPCs (**c**), and in neurons and co-neurons (**d**). **e**, Alluvial plot showing the GO terms for NPCs, co-NPCs, neurons and co-neurons (day 18). The thickness indicates the number of genes per GO term. **f**, Proliferative activity of neuronal cells from day 14 organoid and cocultures ($n = 11$ each). **g**, Volcano plot of proteomic data showing PRPH as highly expressed in co-NPCs compared to NPCs. **h**, Levels of expression of PRPH in neuronal cells from day 18 organoid alone and cocultures. **g**,**h**, $n = 3$ in triplicate. **i**, Left, immunostaining of purified NPCs from day 18 organoids and coculture organoids. Right, axon lengths and numbers for each cell (number of axons measured: $n = 286$ from $n = 493$ NPCs, $n = 628$ from $n = 896$ co-NPCs) ($n = 2$ combined). **j**,**k**, Heatmaps showing the expression of genes involved in neurogenesis, axon development, phagocytosis and neuronal death (**j**) and proteins involved in neurogenesis and axon development preponderant in day 18 iMicro (**k**). **l**,**m**, Coculture organoid (day 18) staining showing iMicro in proximity to TUJ1⁺ neuronal axons ($n = 3$) (**l**) and Ki67⁺SOX2⁺ NPCs ($n = 3$) (**m**). **n**, Detection of SOX2⁺ NPCs in IBA1⁺ iMicro from coculture organoid (day 18, $n = 5$) by immunostaining. Statistical analysis, two-way ANOVA (**a**), Mann–Whitney test (**b**,**f**,**i**), one-way ANOVA (**h**). Error bars, mean ± s.e.m. Scale bars, 300 µm (**a**), 100 µm (**i**), 50 µm (**i**,**m**,**n**), 30 µm (**l**). Adj., adjusted. FC, fold change. *$P \le 0.05$; **$P \le 0.01$; ***$P \le 0.001$; ****$P \le 0.0001$.

molecular changes behind the reduced frequencies of NPCs in cocultured organoids (co-NPCs). With reduced NPC frequencies not directly evident (Extended Data Fig. 5i, j), DEG analysis revealed that cell proliferation genes were significantly less expressed in co-NPCs compared to NPCs, but not in neurons (Fig. 2c,d, Extended Data Fig. 6a,b and Supplementary Table 5). The proliferating zone on the uniform manifold approximation and projection (UMAP) space using cell proliferation genes was dominated by NPCs (Extended Data Fig. 6c), with a

significant reduction in the proportion of dividing co-NPCs (Extended Data Fig. 6d). Indeed co-NPCs (but not co-neurons) presented a significant reduction in EdU labelling (Fig. 2f) and in staining for Ki67 (Extended Data Fig. 6e and Supplementary Video 6), rather than an increased level of cell death (Caspase3) (Extended Data Fig. 6f). Several genes involved in axon development and neurogenesis pathways such as *GAP43* and *NEFM* were also significantly highly expressed in co-NPCs and co-neurons compared to their organoid-only counterparts (Fig. 2c–e, Extended Data Fig. 6a,b and Supplementary Tables 5 and 6).

A proteomic analysis on purified neuronal cells (Supplementary Table 7) then revealed that the expression of the neuronal axon filament protein PRPH[38] was markedly higher in co-NPCs (reaching the levels observed in co-neurons) (Fig. 2g,h and Supplementary Table 8), while co-NPCs exhibited significantly more and longer neurites than NPCs from organoids alone (Fig. 2i). This demonstrated that iMicro triggered marked organoid remodelling, with differentiating NPCs favouring axon development instead of proliferation, typical of neuronal cells undergoing maturation (Fig. 2e). In addition, genes expressed at lower levels in cocultured organoids than organoids alone are highly expressed during the early stages of human brain development (8–9 postconceptual weeks (pcw))[39] while those at higher levels in cocultured organoids are typically highly expressed at later stages of brain development (37 pcw). Altogether, iMicro seem to promote the maturation of brain organoids (Supplementary Fig. 3). Accordingly, genes and proteins driving neurogenesis and neuronal axon development by microglia were expressed at significantly higher levels in iMicro compared to iMac (Fig. 2j,k and Extended Data Fig. 3a,b).

Embryonic microglia contribute to neurogenesis by selectively colonizing the proliferative zones in the cerebral cortex and phagocytosing neural precursor cells[2], while participating in neuronal development by engulfing and remodelling neuronal synapses postnatally[40]. Indeed, genes involved in phagocytosis were expressed at higher levels in iMicro than iMac (Fig. 2j). While iMicro and co-NPCs were in close contact (Supplementary Video 7), some of the iMicro near Ki67$^+$ NPCs exhibited traces of SOX2$^+$ NPCs (Fig. 2l,m), and IBA1$^+$ iMicro had engulfed traces of TUJ1$^+$ neurons next to which they also localized (Fig. 2n, Extended Data Fig. 5k,l and Supplementary Videos 1 and 8). Altogether, this suggest that iMicro contribute to the reduction of NPC proliferative activity, while promoting their maturation and axonogenesis in organoid cocultures.

These results, alongside the Ki67 staining being restricted to NPC-enriched areas (Extended Data Figs. 6e and 7a and Supplementary Video 6), led us to study neural rosettes[41], which appeared smaller, disorganized and surrounded by iMicro in cocultured organoids (Extended Data Fig. 7a–c and Supplementary Video 9). We compared proteomic analysis of microdissected neural rosettes from organoids and coculture organoids (Extended Data Fig. 7d and Supplementary Table 9) with proteomic analysis of purified NPCs, co-NPCs, neurons and co-neurons (Supplementary Table 7), and unravelled a clear signature associated with neurogenesis, axonogenesis, glial cell differentiation and reduced proliferation preponderant in neural rosettes from coculture organoids (Extended Data Fig. 7d,e).

iMicro provide cholesterol and its esters to NPCs

We then explored the mechanisms that drive iMicro's effect on cocultured organoids. DEG between iMicro and iMac (Supplementary Table 1) revealed that iMicro presented remodelled lipid metabolism pathways with several genes involved in cholesterol transport and storage including *ABCA1*, *ABCG1* or *PLIN2* highly expressed in iMicro (Extended Data Fig. 3a). The strongest DEG *PLIN2*, a hallmark of lipid droplets (Fig. 3a), was highly expressed at the protein level in iMac (Fig. 3b). iMicro are also the major cell type in cocultured organoids exhibiting PLIN2$^+$ lipid droplets colocalizing with neutral lipids (Fig. 3c,d and Supplementary Video 10). This observation directed us to the biology of lipid droplets and associated cholesterol pathways, which were negatively regulated in iMac in our differentially expressed protein analysis between iMac and iMicro (Extended Data Fig. 8a). Co-NPCs also contained significantly higher levels of neutral lipids compared to NPCs, despite neither co-NPCs nor co-neurons displaying any enrichment in pathways involved in cholesterol biosynthesis at the protein level[42] (Fig. 3e and Extended Data Fig. 8b,c).

We hypothesized that iMicro can export cholesterol to neuronal cells in organoids. iMac could uptake fluorescent cholesterol-ester C12 (BODIPY^{CE}), integrate it into to PLIN2$^+$ lipid droplets (Fig. 3f) before transferring it to co-NPCs during coculture (Fig. 3g). Such transfer required BODIPY^{CE} to originate from iMicro as NPCs from organoid alone were not able to take up free BODIPY^{CE} (Fig. 3h), but did not require physical contact between iMicro and neuronal cells (Fig. 3i). We could also partially mimic the action of iMicro on the size of organoid coculture by transferring iMac-conditioned medium (Fig. 3j and Extended Data Fig. 8d,e,f), with a lipid composition similar to that of medium of coculture organoids, but enriched in phospholipids, cholesterol and cholesteryl-esters (Fig. 3k, Extended Data Fig. 9a and Supplementary Table 10).

In addition, our proteomic data revealed that APOE and AIBP (apolipoprotein 1 binding protein) were highly expressed in iMac (Fig. 3l), which secreted high levels of APOE in the culture medium (Extended Data Fig. 9b and Supplementary Fig. 1a). Alongside the specific lipid profile of iMac conditioned media, this signature suggested that cholesterol and its esters originated from iMac and were transported to neuronal cells via APOE$^+$ lipoprotein-like particles (LPLs)[43]; especially as high levels of APOE proteins were detected in co-NPCs not expressing its transcript (Extended Data Fig. 9c). We indeed detected high levels of APOE in the culture medium of coculture organoids, but not of organoids alone, further confirming that it originated from iMicro (Fig. 3m, Extended Data Fig. 9d and Supplementary Fig. 1b,c); its restriction to the high-density lipoprotein (HDL)-enriched fraction suggested that APOE$^+$ LPLs resembled HDL (Extended Data Fig. 9e and Supplementary Fig. 1d).

The expression of AIBP facilitating the efflux of cholesterol by the ATP-binding-cassette receptor and cholesterol transporter ABCA1 for integration into APOE/APOA1 LPLs prompted us to explore the function of ABCA1, which was highly expressed by iMac and iMicro at transcript and protein levels, but not expressed by co-NPCs and co-neurons[44–47] (Fig. 3n and Extended Data Fig. 9f). Inhibition of ABCA1 with probucol led to the accumulation of LipidSpot 610$^+$ lipid droplets in iMac[48,49] (Fig. 3o) and prevented the esterification and thus the further integration of cholesterol released through ABCA1 into APOE$^+$ HDL. This was reflected in lipid content of the culture medium of treated iMac also showing a reduction in the level of phospholipids and an increase in triglycerides[45,46] (Fig. 3p, Extended Data Fig. 9g and Supplementary Table 11). The blocking of ABCA1 using probucol significantly abrogated the transfer of cholesterol into co-NPCs (Fig. 3q) and the subsequent reduction of size in coculture organoids (Fig. 3r and Extended Data Fig. 9h), while abrogating the decreased proliferation of co-NPCs previously observed (Fig. 3s). Altogether, these data strongly suggest that iMac/iMicro transport cholesterol and its esters to neuronal cells in cocultured organoids, potentially via APOE LPLs resembling HDL.

PLIN2$^+$ microglia are present in fetal brains

To validate these findings in vivo, we first explored publicly available expression datasets of mouse microglia from different stages of development from embryonic day (E) 10.5 to adulthood[50]. Mouse microglia highly expressed genes involved in cholesterol biosynthesis, transport and lipid storage during early brain development, with their expression almost absent in adult mice (Fig. 4a). The same trend was present in human microglia (Extended Data Fig. 10a). Lipid droplet-rich

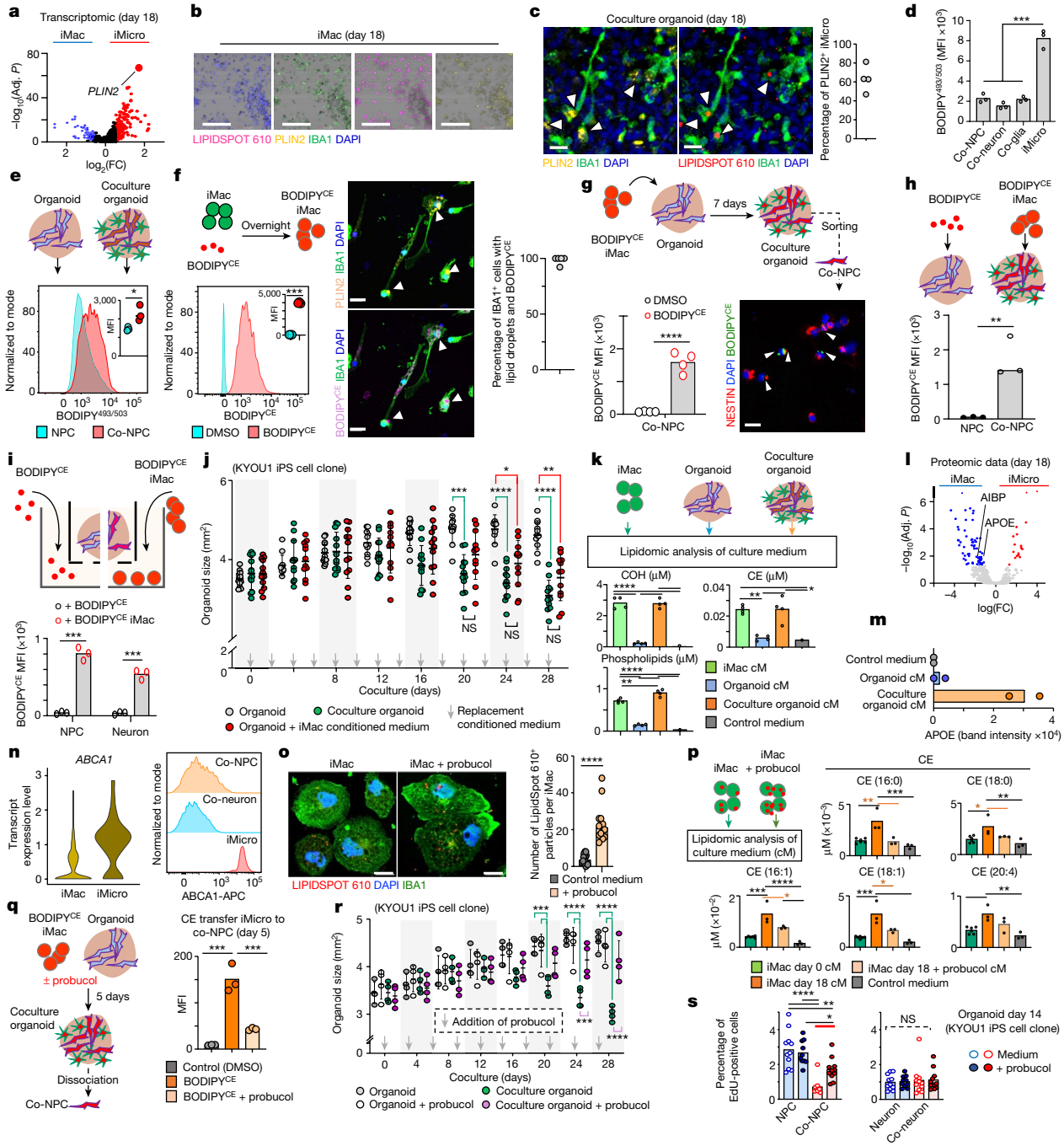

Fig. 3 | Lipid-enriched iMicro transport cholesterol and cholesterol-esters to neuronal cells in organoids. a, *PLIN2* is the highest DEG overexpressed in day 18 iMicro. **b**, Staining of IBA1$^+$ iMac for PLIN2 and LipidSpot 610 ($n = 4$). **c**, Staining of day 18 cocultured organoid for IBA1, DAPI, PLIN2 and LipidSpot 610 ($n = 4$). **d**, Neutral-lipid (BODIPY$^{493/503+}$) levels in day 18 co-glial, iMicro, co-neural cells by flow cytometry ($n = 3$). **e**, Neutral-lipid levels in NPCs and co-NPCs (flow cytometry, $n = 3$). **f**, Integration of cholesterol-esters by iMac pulsed overnight with BODIPY^{CE} (flow cytometry, $n = 3$; PLIN2 costaining, $n = 5$). **g**, BODIPY^{CE+} iMicro transfer cholesterol-esters to co-NPCs in organoids within 7 days (flow cytometry, $n = 3$; immunofluorescence on co-NPCs, $n = 4$). **h**, Co-NPC ability to take-up cholesterol-esters ($n = 3$). **i**, Transfer of cholesterol-esters from iMicro to neuronal cells in organoids ($n = 3$, transwell). **j**, Effect of iMac conditioned medium (cM) on organoid size ($n = 3$ experiments, $n = 12$ samples). **k**, Lipid profiles of cM from iMac and organoids ($n = 4$; controls, $n = 2$). **l**, AIBP and APOE as key differentially expressed proteins between iMac and iMicro (day 18). **m**, APOE levels in the cM of day 18 organoids ($n = 2$ each, western blot). **n**, Expression levels of *ABCA1* between iMac and iMicro (day 18, $n = 3$) (left) and of ABCA1 by iMicro, co-NPC and co-neuron (day 18, one of several observations) (right). **o**–**q**, Effect of ABCA1 inhibitor (probucol) on LipidSpot 610 staining of day 18 IBA1$^+$ iMac ($n = 14$) (**o**), the levels of cholesteryl-esters in iMac cM ($n = 3$) (**p**) and their transfer from BODIPY^{CE+} iMicro to co-NPCs (day 18, $n = 3$) (**q**). **r**,**s**, Effect of probucol on the size of organoids (**r**) (three independent experiments, $n = 4$ each) and the proliferative activity of NPCs and neurons in day 14 organoids ($n = 11$ each) (**s**). Statistical analysis, two-way ANOVA (**j**,**r**), one-way ANOVA (**d**,**k**,**p**,**q**,**s**), Mann–Whitney test (**e**–**i**,**o**). Error bars: mean ± s.e.m. Scale bars, 15 μm (**c**), 30 μm (**f**), 25 μm (**g**). *$P \le 0.05$; **$P \le 0.01$; ***$P \le 0.001$; ****$P \le 0.0001$. Asterisks above horizontal bars apply to all bars beneath them. MFI, median fluorescent intensity.

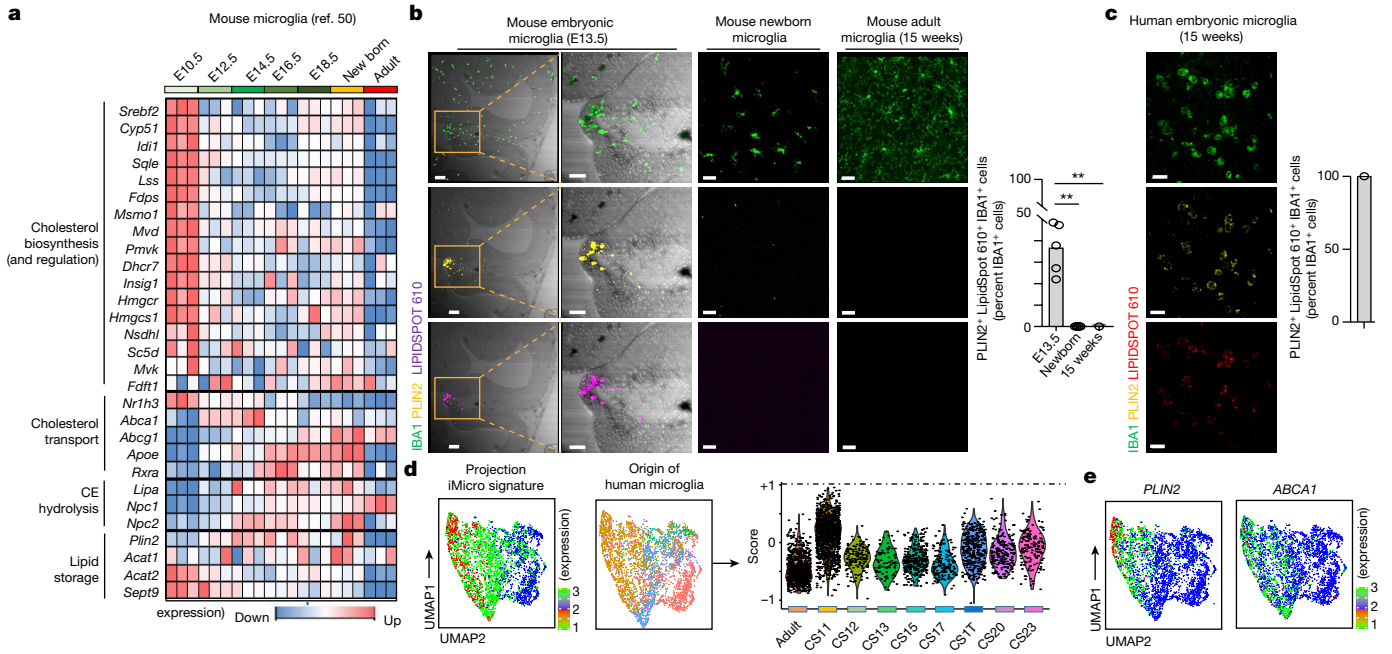

Fig. 4 | Embryonic microglia express APOE, PLIN2 and high levels of neutral lipid. a, Heatmap of genes involved in cholesterol metabolism in mouse microglia through fetal development until adulthood. **b**, Staining of E13.5 roof plate region of embryonic ($n = 5$), newborn ($n = 4$) and 15-week-old ($n = 5$) mouse brains for IBA1, PLIN2 and LipidSpot 610. **c**, Staining of 15-weeks-of-gestation human embryonic brains for IBA1, PLIN2 and LipidSpot 610. (One of several observations). In **b**,**c**, graphs represents the proportion of IBA1$^+$ cells expressing PLIN2 and presenting staining for LipidSpot 610 (quantification of $n = 3$ images in each case). Mean is represented. **d**, Projection of iMicro (day 18) onto UMAP clustering of human fetal and adult microglia transcriptome data and associated identity scores. **e**, Expression of *PLIN2* and *ABCA1* on UMAP of human fetal microglia. **d** and **e** use data from the Allen human brain atlas. Statistical analysis, one-way ANOVA (**b**). Scale bars, 200 µm (**b**, left panels), 100 µm (**b**, boxes in left panels), 50 µm (**c**), 30 µm (**b**), middle and right panels).

microglial cells were detected in mouse embryonic brain at E13.5/E14.5, but not in newborn and adult mouse brain (Fig. 4b and Extended Data Fig. 10b). Similarly, brain from 15- to 21-week-old human embryos also contained lipid droplet-rich microglial cells (Fig. 4c and Extended Data Fig. 10e). Integrating our scRNA-seq data with previously published human microglia scRNA-seq data from both embryonic[51] and adult[39] stages showed that iMicro in our organoid coculture model at day 18 resemble those of CS11 human embryonic microglia (Fig. 4d), with *PLIN2* and *ABCA1* transcripts exclusively detectable in early CS11 embryonic stages and absent at later stages of development (Fig. 4e). Meanwhile, transcriptomic analysis of E14.5 mouse brain[51] showed that, like iMicro, embryonic microglia expressed the highest level of genes involved in lipid storage, cholesterol esterification and transport compared to the other cell types in the brain (Extended Data Fig. 10c,d). In particular, the high expression of *ABCA1*, *ABCG1*, *PLIN2* and *APOE* in mouse and human embryonic microglia suggested that they also have the potential to transport cholesterols to neuronal cells in the developing brain (Fig. 4a and Extended Data Fig. 10a,c,d). Altogether, these data suggest that iMicro recapitulate a key feature of embryonic microglia, representing a major source of cholesterols, stored in their lipid droplets ready for export and uptake by neuronal cells.

Discussion

Much of our current knowledge of neurogenesis is based on studies in animal models owing to limited access to human fetuses. One way of overcoming this limitation is the use of organoid cultures, and here we used human iPS cells to generate brain organoids mimicking the early stages of brain development in embryos. Previous brain organoid models have been limited by the lack of vasculature, although some progress towards this is being made[52], and the lack of microglia. Although several studies have attempted to incorporate microglia into brain organoid models and other models, they did not precisely study macrophage to microglia differentiation nor address the crosstalk between microglia and neuronal cells[19–21]. Here, we further advanced the brain organoid model by coculturing iMac derived from the same iPS cell, thereby attempting to model the arrival of the first wave of microglia reaching the brain from the yolk-sac[1]. iMac slowly embedded into the brain organoid and displayed phenotype and functions resembling those described in microglia. The presence of iMicro in cocultured organoids enhanced neurogenesis both phenotypically and functionally, illustrating the potential for using this model to dissect early human brain development and, in the future, to model the onset of microglia-driven neurodegenerative diseases. This latter point is of critical importance given that the presence of altered microglia, such as those in individuals with TREM2 and APOE polymorphism, is linked with increased susceptibility to Alzheimer's disease[53,54].

We also saw that genes involved in hypoxia, pro-angiogenesis and immune response are expressed at higher levels in both neuronal cells and iMicro in coculture organoids compared to organoids alone. This implies that the first wave of microglia may have an important role in the developing vasculature of the brain and in immune defence against postnatal challenges. An important observation we made was the significant reduction in the size of the organoids upon coculture with iMac, due to reduced NPC proliferation. Many tissues, including the brain, undergo rapid growth during the early stages of embryonic development. It is interesting to postulate that when primitive macrophages occupy the tissues, they might help to protect against excessive growth and thereby preserve proper embryogenesis, unravelling a unique crosstalk between tissue stem cells and macrophages.

Realizing that iMicro possess a higher lipid metabolism and especially cholesterol metabolism compared to iMac, we attempted to understand how this might influence iMicro's modulation of neurogenesis. iMicro are an important source of cholesterol for co-NPCs. The lipidomic analysis and the high expression of ABCA1, AIBP and APOE in iMac and iMicro suggest that the transport of cholesterol and its esters

is an active process mediated by lipoprotein particles resembling HDL. Although the mechanism is still elusive and under study, the transported cholesterol and its esters would then be utilized by neuronal cells and be involved in the improved neurogenesis we observed in the presence of iMicro. Indeed, the blocking of ABCA1 abrogated the reduction of size of organoid cocultured with iMac, a phenomenon associated with a marked decrease in cholesteryl-esters.

This finding, which was validated using various human iPS cell lines (Supplementary Table 4), is particularly important as previous studies have shown that astrocytes (which are not yet present in the embryonic brain) are the major cell type in the adult brain that produce cholesterols, and are required for proper neurite outgrowth and synapse formation[55,56]. The transportation of cholesterol from astrocytes to neurons is driven by APOE particles via the low-density lipoprotein (LDL) receptor[56–58]. Based on our discovery of lipid-enriched PLIN2$^+$ iMicro and embryonic microglia that highly express APOE, AIBP and ABCA1, we hypothesize that during early brain development, when astrocytes are absent, it is microglia that produce and export the necessary cholesterol species to neuronal cells potentially via APOE$^+$ LPLs resembling HDL.

It would then remain that the arrival of the first wave of microglia, which we mimic in our organoid, is critical for the large-scale remodelling of the brain as well as for synaptic pruning and axonogenesis, and perhaps also for supporting development of the vasculature[1,59,60]. One contribution of microglia is also through their ability to provide developing co-NPCs with the lipid and cholesterol sources they require. The roles of lipids in the brain go beyond myelin formation, neurite outgrowth and synapse formation, and include substantial influence on the proliferation and neurogenesis of NPCs[60–63]. Our model mimicking the early stages of neurogenesis suggests that lipid and cholesterol species derived from iMicro have a key role in the proliferation and differentiation of co-NPCs that we observed. Thus, our study describes an important tool to better understand the ontogeny and roles of these iPS cell-derived microglia in early neurogenesis.

Beyond the case of brain organoids, our approach supports the notion that addition of resident macrophages to organoids changes their physiology and differentiation, and therefore should be tested in other organoids. This is important and timely as there is much interest in organoids, as exemplified by the call to establish an 'Organoid Cell Atlas' within the global Human Cell Atlas initiative, which aims to combine single-cell profiling with organoid technology and holds the potential for exciting advances in our understanding of human tissues and organ processes.

Online content

Any methods, additional references, Nature Portfolio reporting summaries, source data, extended data, supplementary information, acknowledgements, peer review information; details of author contributions and competing interests; and statements of data and code availability are available at https://doi.org/10.1038/s41586-023-06713-1.

1. Ginhoux, F. et al. Fate mapping analysis reveals that adult microglia derive from primitive macrophages. *Science* **330**, 841–845 (2010).
2. Cunningham, C. L., Martinez-Cerdeno, V. & Noctor, S. C. Microglia regulate the number of neural precursor cells in the developing cerebral cortex. *J. Neurosci.* **33**, 4216–4233 (2013).
3. Marin-Teva, J. L., Cuadros, M. A., Martin-Oliva, D. & Navascues, J. Microglia and neuronal cell death. *Neuron Glia Biol.* **7**, 25–40 (2011).
4. Sierra, A. et al. Microglia shape adult hippocampal neurogenesis through apoptosis-coupled phagocytosis. *Cell Stem Cell.* **7**, 483–495 (2010).
5. Shigemoto-Mogami, Y., Hoshikawa, K., Goldman, J. E., Sekino, Y. & Sato, K. Microglia enhance neurogenesis and oligodendrogenesis in the early postnatal subventricular zone. *J. Neurosci.* **34**, 2231–2243 (2014).
6. Squarzoni, P. et al. Microglia modulate wiring of the embryonic forebrain. *Cell Rep.* **8**, 1271–1279 (2014).
7. Lancaster, M. A. & Knoblich, J. A. Generation of cerebral organoids from human pluripotent stem cells. *Nat. Protoc.* **9**, 2329–2340 (2014).
8. Lancaster, M. A. et al. Cerebral organoids model human brain development and microcephaly. *Nature* **501**, 373–379 (2013).
9. Pasca, A. M. et al. Functional cortical neurons and astrocytes from human pluripotent stem cells in 3D culture. *Nat. Methods* **12**, 671–678 (2015).
10. Qian, X. et al. Brain-region-specific organoids using mini-bioreactors for modeling ZIKV exposure. *Cell* **165**, 1238–1254 (2016).
11. Quadrato, G. et al. Cell diversity and network dynamics in photosensitive human brain organoids. *Nature* **545**, 48–53 (2017).
12. Camp, J. G. et al. Human cerebral organoids recapitulate gene expression programs of fetal neocortex development. *Proc. Natl Acad. Sci. USA* **112**, 15672–15677 (2015).
13. Kelava, I. & Lancaster, M. A. Dishing out mini-brains: current progress and future prospects in brain organoid research. *Dev. Biol.* **420**, 199–209 (2016).
14. Qian, X., Song, H. & Ming, G. L. Brain organoids: advances, applications and challenges. *Development* **146**, dev166074 (2019).
15. Lee, C. Z. W., Kozaki, T. & Ginhoux, F. Studying tissue macrophages in vitro: are iPSC-derived cells the answer? *Nat. Rev. Immunol.* **18**, 716–725 (2018).
16. Monier, A. et al. Entry and distribution of microglial cells in human embryonic and fetal cerebral cortex. *J. Neuropathol. Exp. Neurol.* **66**, 372–382 (2007).
17. Bian, Z. et al. Deciphering human macrophage development at single-cell resolution. *Nature* **582**, 571–576 (2020).
18. Kanton, S. et al. Organoid single-cell genomic atlas uncovers human-specific features of brain development. *Nature* **574**, 418–422 (2019).
19. Popova, G. et al. Human microglia states are conserved across experimental models and regulate neural stem cell responses in chimeric organoids. *Cell Stem Cell* **28**, 2153–66 e6 (2021).
20. Xu, R. et al. Developing human pluripotent stem cell-based cerebral organoids with a controllable microglia ratio for modeling brain development and pathology. *Stem Cell Reports* **16**, 1923–1937 (2021).
21. Schafer, S. T. et al. An in vivo neuroimmune organoid model to study human microglia phenotypes. *Cell* **186**, 2111–2126 e20 (2023).
22. Takata, K. et al. Induced-pluripotent-stem-cell-derived primitive macrophages provide a platform for modeling tissue-resident macrophage differentiation and function. *Immunity* **47**, 183–198 e6 (2017).
23. Bohlen, C. J. et al. Diverse requirements for microglial survival, specification, and function revealed by defined-medium cultures. *Neuron* **94**, 759–773 e8 (2017).
24. Gosselin, D. et al. An environment-dependent transcriptional network specifies human microglia identity. *Science* **356**, eaal3222 (2017).
25. Su, N. et al. Occurrence of transmembrane protein 119 in the retina is not restricted to the microglia: an immunohistochemical study. *Transl. Vis. Sci. Technol.* **8**, 29 (2019).
26. Vankriekelsvenne, E. et al. Transmembrane protein 119 is neither a specific nor a reliable marker for microglia. *Glia* **70**, 1170–1190 (2022).
27. Bennett, M. L. et al. New tools for studying microglia in the mouse and human CNS. *Proc. Natl Acad. Sci. USA* **113**, E1738–1746 (2016).
28. Nimmerjahn, A., Kirchhoff, F. & Helmchen, F. Resting microglial cells are highly dynamic surveillants of brain parenchyma in vivo. *Science* **308**, 1314–1318 (2005).
29. Lee, C. Y. & Landreth, G. E. The role of microglia in amyloid clearance from the AD brain. *J. Neural Transm. (Vienna)* **117**, 949–960 (2010).
30. Butler, A., Hoffman, P., Smibert, P., Papalexi, E. & Satija, R. Integrating single-cell transcriptomic data across different conditions, technologies, and species. *Nat. Biotechnol.* **36**, 411–420 (2018).
31. Aibar, S. et al. SCENIC: single-cell regulatory network inference and clustering. *Nat. Methods* **14**, 1083–1086 (2017).
32. Fagerlund, I. et al. Microglia-like cells promote neuronal functions in cerebral organoids. *Cells.* **11**, 124 (2021).
33. Abud, E. M. et al. iPSC-derived human microglia-like cells to study neurological diseases. *Neuron* **94**, 278–293 e9 (2017).
34. Ormel, P. R. et al. Microglia innately develop within cerebral organoids. *Nat. Commun.* **9**, 4167 (2018).
35. Kierdorf, K. et al. Microglia emerge from erythromyeloid precursors via Pu.1- and Irf8-dependent pathways. *Nat. Neurosci.* **16**, 273–280 (2013).
36. Herbomel, P., Thisse, B. & Thisse, C. Zebrafish early macrophages colonize cephalic mesenchyme and developing brain, retina, and epidermis through a M-CSF receptor-dependent invasive process. *Dev. Biol.* **238**, 274–288 (2001).
37. Yuan, S. H. et al. Cell-surface marker signatures for the isolation of neural stem cells, glia and neurons derived from human pluripotent stem cells. *PLoS ONE* **6**, e17540 (2011).
38. Portier, M. M., Escurat, M., Landon, F., Djabali, K. & Bousquet, O. Peripherin and neurofilaments: expression and role during neural development. *C. R. Acad. Sci. III* **316**, 1124–1140 (1993).
39. Hawrylycz, M. J. et al. An anatomically comprehensive atlas of the adult human brain transcriptome. *Nature* **489**, 391–399 (2012).
40. Favuzzi, E. et al. GABA-receptive microglia selectively sculpt developing inhibitory circuits. *Cell* **184**, 5686 (2021).
41. Townshend, R. F. et al. Effect of cell spreading on rosette formation by human pluripotent stem cell-derived neural progenitor cells. *Front. Cell. Dev. Biol.* **8**, 588941 (2020).
42. Bengoechea-Alonso, M. T. & Ericsson, J. SREBP in signal transduction: cholesterol metabolism and beyond. *Curr. Opin. Cell Biol.* **19**, 215–222 (2007).
43. Kontush, A., Lhomme, M. & Chapman, M. J. Unraveling the complexities of the HDL lipidome. *J. Lipid Res.* **54**, 2950–2963 (2013).
44. Chroni, A., Liu, T., Fitzgerald, M. L., Freeman, M. W. & Zannis, V. I. Cross-linking and lipid efflux properties of apoA-I mutants suggest direct association between apoA-I helices and ABCA1. *Biochemistry* **43**, 2126–2139 (2004).
45. Chung, S. et al. Targeted deletion of hepatocyte ABCA1 leads to very low density lipoprotein triglyceride overproduction and low density lipoprotein hypercatabolism. *J. Biol. Chem.* **285**, 12197–12209 (2010).

46. Kypreos, K. E. ABCA1 promotes the de novo biogenesis of apolipoprotein CIII-containing HDL particles in vivo and modulates the severity of apolipoprotein CIII-induced hypertriglyceridemia. *Biochemistry* **47**, 10491–10502 (2008).
47. Smith, J. D. et al. ABCA1 mediates concurrent cholesterol and phospholipid efflux to apolipoprotein A-I. *J. Lipid Res.* **45**, 635–644 (2004).
48. Favari, E. et al. Probucol inhibits ABCA1-mediated cellular lipid efflux. *Arterioscler. Thromb. Vasc. Biol.* **24**, 2345–2350 (2004).
49. Jin, X. et al. ABCA1 contributes to macrophage deposition of extracellular cholesterol. *J. Lipid Res.* **56**, 1720–1726 (2015).
50. Thion, M. S. et al. Microbiome influences prenatal and adult microglia in a sex-specific manner. *Cell* **172**, 500–516 e16 (2018).
51. Loo, L. et al. Single-cell transcriptomic analysis of mouse neocortical development. *Nat. Commun.* **10**, 134 (2019).
52. Cakir, B. et al. Engineering of human brain organoids with a functional vascular-like system. *Nat. Methods* **16**, 1169–1175 (2019).
53. Jansen, I. E. et al. Genome-wide meta-analysis identifies new loci and functional pathways influencing Alzheimer's disease risk. *Nat. Genet.* **51**, 404–413 (2019).
54. Kunkle, B. W. et al. Genetic meta-analysis of diagnosed Alzheimer's disease identifies new risk loci and implicates Abeta, tau, immunity and lipid processing. *Nat. Genet.* **51**, 414–430 (2019).
55. Ferris, H. A. et al. Loss of astrocyte cholesterol synthesis disrupts neuronal function and alters whole-body metabolism. *Proc. Natl Acad. Sci. USA* **114**, 1189–1194. (2017).
56. Mauch, D. H. et al. CNS synaptogenesis promoted by glia-derived cholesterol. *Science* **294**, 1354–1357 (2001).
57. Ioannou, M. S. et al. Neuron-astrocyte metabolic coupling protects against activity-induced fatty acid toxicity. *Cell* **177**, 1522–1535 e14 (2019).
58. Ito, J., Nagayasu, Y., Miura, Y., Yokoyama, S. & Michikawa, M. Astrocytes endogenous apoE generates HDL-like lipoproteins using previously synthesized cholesterol through interaction with ABCA1. *Brain Res.* **1570**, 1–12 (2014).
59. Hughes, A. N. & Appel, B. Microglia phagocytose myelin sheaths to modify developmental myelination. *Nat. Neurosci.* **23**, 1055–1066 (2020).
60. Scott-Hewitt, N. et al. Local externalization of phosphatidylserine mediates developmental synaptic pruning by microglia. *EMBO J.* **39**, e105380 (2020).
61. Knobloch, M. The role of lipid metabolism for neural stem cell regulation. *Brain Plast.* **3**, 61–71 (2017).
62. Driver, A. M., Kratz, L. E., Kelley, R. I. & Stottmann, R. W. Altered cholesterol biosynthesis causes precocious neurogenesis in the developing mouse forebrain. *Neurobiol. Dis.* **91**, 69–82 (2016).
63. Knobloch, M. et al. Metabolic control of adult neural stem cell activity by Fasn-dependent lipogenesis. *Nature* **493**, 226–230 (2013).

[1]Singapore Immunology Network (SIgN), Agency for Science, Technology and Research, Singapore, Singapore. [2]Department of Microbiology and Immunology, Yong Loo Lin School of Medicine, National University of Singapore, Singapore, Singapore. [3]INSERM U1015, Gustave Roussy Cancer Campus, Villejuif, France. [4]Department of Biochemistry, Yong Loo Lin School of Medicine, National University of Singapore, Singapore, Singapore. [5]Singapore Lipidomics Incubator (SLING), Life Sciences Institute, National University of Singapore, Singapore, Singapore. [6]Institut de Biologie de l'Ecole Normale Supérieure (IBENS), Ecole Normale Supérieure, CNRS, INSERM, PSL Research University, Paris, France. [7]Functional Proteomics Laboratory, SingMass National Laboratory, Institute of Molecular and Cell Biology, Agency for Science, Technology and Research, Singapore, Singapore. [8]Translational Immunology Institute, SingHealth Duke-NUS Academic Medical Centre, Singapore, Singapore. [9]Translational Laboratory in Genetic Medicine (TLGM), Agency for Science, Technology and Research, Singapore, Singapore. [10]Institute of Molecular and Cell Biology (IMCB), Agency for Science, Technology and Research, Singapore, Singapore. [11]Oncoprot Platform, TBM-Core US 005, Bordeaux, France. [12]Bordeaux Protéome, University of Bordeaux, Bordeaux, France. [13]Wellcome Trust-Medical Research Council Cambridge Stem Cell Institute and Department of Veterinary Medicine, University of Cambridge, Cambridge, UK. [14]A*STAR Microscopy Platform Electron Microscopy, Research Support Centre, Agency for Science, Technology and Research (A*STAR), Singapore, Singapore. [15]Shanghai Institute of Immunology, Department of Immunology and Microbiology, Shanghai Jiao Tong University School of Medicine, Shanghai, China. [16]Shanghai Immune Therapy Institute, Renji Hospital, Shanghai Jiao Tong University School of Medicine, Shanghai, China. [17]INSERM U981, Molecular Predictors and New Targets in Oncology & Département de Cancérologie de l'Enfant et de l'Adolescent, Gustave Roussy, Université Paris-Saclay, Villejuif, France. [18]Department of Reproductive Medicine, KK Women's and Children's Hospital, Singapore, Singapore. [19]Department of Medical Science, College of Medicine, CHA University, Seongnam, Republic of Korea. [20]Department of Medical Genetics, Centre for Molecular Medicine and Therapeutics, Djavad Mowafaghian Centre for Brain Health, University of British Columbia, Vancouver, British Columbia, Canada. [21]British Columbia Children's Hospital Research Institute, Vancouver, British Columbia, Canada. [22]School of Biosciences, Faculty of Health and Medical Sciences, University of Surrey, Guildford, UK. [23]These authors contributed equally: Dong Shin Park, Tatsuya Kozaki. ✉e-mail: florent_ginhoux@immunol.a-star.edu.sg

Methods

Reprogramming of patient-derived fibroblasts into induced pluripotent stem cell culture

To isolate and culture fibroblasts, skin samples from paediatric patients with high-grade glioma were collected during a surgical procedure for care purpose (that is, central venous catheter placement, tumour biopsy/surgery, ventriculoperitoneal shunt and so on). Fibroblasts were cultured in Dulbecco's Modified Eagle's medium (DMEM) (Gibco, catalogue no. 11966025) with 1% GlutaMAX-I (100×; Thermo Scientific, catalogue no. 35050038), 1% Sodium Pyruvate (Gibco, catalogue no. 11360070), 1% MEM Non-Essential Amino Acids Solution (100×; Gibco, catalogue no. 11140035), 1% penicillin/streptomycin (10,000 U ml^{-1}; Gibco, catalogue no. 15140122) and 10% fetal bovine serum, ES Cell Qualified One Shot (Gibco, catalogue no. 16141079). At 80% confluence, fibroblasts were electroporated using the Lonza 4D-Nucleofector (Lonza, catalogue no. AAF-1002B) with the episomal iPS cell reprogramming vector (Invitrogen, catalogue no. A14703) according to manufacturer's instructions and plated on Matrigel (Corning, catalogue no. 354277)-coated six-well plates (day 1). From day 0 until day 15 posttransfection, cells were maintained in N2B27 medium containing DMEM/F-12 (Gibco, catalogue no. 21331020), 1% N-2 Supplement (100×; Gibco, catalogue no. 17502048), 2% B-27 supplement Plus Gibco (50×; Gibco, catalogue no. A3582801), 1% HEPES (1 M; Gibco, catalogue no. 15630106), 1% GlutaMAX-I (100×; Thermo Scientific, catalogue no. 35050038), 1% MEM Non-Essential Amino Acids Solution (100×; Gibco, catalogue no. 11140035) and 0.1% β-mercaptoethanol (x1,000) (55 mM; Gibco, catalogue no. 21985023). The N2B27 medium was supplemented with the following cytokines, freshly added: PD0325901 (Biotechne, catalogue no. 4192) 0.5 µM; CHIR99021 (Biotechne, catalogue no. 4423) 3 µM; Human Leukemia Inhibitory Factor (Sigma-Aldrich, catalogue no. LIF1010) 10 ng ml^{-1}; A-83-01 (Biotechne, catalogue no. 2939) 0.5 µM; ROCk inhibitor (Sigma-Aldrich, catalogue no. SCM075) 10 µM; and Basic Fibroblast Growth Factor (Biotechne, catalogue no. 233-FB) 100 ng ml^{-1}. From day 15 after transfection, cells were maintained in mTeSR1 medium (STEMCELL Technologies, catalogue no. 85850), which was changed every other day. When iPS cells colonies reached the appropriate size, they were isolated and transferred using a 200 µl pipette into a freshly prepared Matrigel-coated 24-well plate for amplification. The number of organoid/batches used for each of the iPS cells generated from paediatric patients and from commercial/collaborative sources in this study is described in Supplementary Table 4.

Reagents

Composition of culture medium and reagents (antibodies, chemicals and proteins) are listed in Supplementary Tables 1 and 2 respectively.

Induced pluripotent stem cell culture

Human iPS cell KYOU1 (KYOU-DXR0109B, catalogue no. ACS-1023) and IMR-90 (catalogue no. CCL-186) were obtained from ATCC. CTRL iPS cell line was obtained from R. T. Karadottir. CAU iPS cell was obtained from Atlantis Bioscience (catalogue no. pCi-KER_KIT), HD33i from the NINDS iPS cell Repository at Coriell Institute (catalogue no. ND36997), pCi-ASI from Phenocell (catalogue no. pCi-ASI_0.5 M) and XCL-1 from XCell Science (catalogue no. IP-001-1V). All iPS cell lines had verified pluripotency and were mycoplasma-free. The cells were maintained on Matrigel (Corning, catalogue no. 354277) in mTeSR1 medium (STEMCELL Technologies, catalogue no. 85850), which was changed every day. When iPS cells reached about 70% confluence, the cells were passaged using ReLeSR (STEMCELL Technologies, catalogue no. 05872). Unless specified, the KYOU1 iPS cell line is used throughout the manuscript to generate iMac and brain organoids. The number of organoid/batches used for each iPS cell in this study is described in Supplementary Table 4. All cell lines used were checked against the list of commonly misidentified cell lines maintained by the International Cell Line Authentication Committee.

Generation of iMac

iMac were generated as described in ref. 22. In brief, to promote cell commitment towards a primitive streak-like population, and subsequently to the mesoderm cell lineage and into hemangioblasts, human iPS cells were cultured in Stempro medium supplemented with BMP4 (5 ng ml^{-1}), CHIR99021 (2 µM) and VEGF (50 ng ml^{-1}) on day 0. The cells were cultured in Stempro medium supplemented with BMP4 (5 ng ml^{-1}), FGF2 (20 ng ml^{-1}) and VEGF (50 ng ml^{-1}) on day 2. The cells were cultured in Stempro medium supplemented with FGF2 (5 ng ml^{-1}) and VEGF (15 ng ml^{-1}) on day 4. From day 6 to 11, the cells were cultured in Stempro medium supplemented with FGF2 (10 ng ml^{-1}), VEGF (10 ng ml^{-1}), SCF (50 ng ml^{-1}), IL-3 (20 ng ml^{-1}), IL-6 (10 ng ml^{-1}) and DKK1 (30 ng ml^{-1}) to induce hematopoietic cell commitment. The addition of DKK1, a Wnt antagonist, served to promote primitive haematopoiesis. From day 11 to day 15, the cells were cultured in Stempro medium supplemented with FGF2 (10 ng ml^{-1}), IL-3 (20 ng ml^{-1}), IL-6 (10 ng ml^{-1}) and SCF (50 ng ml^{-1}) to differentiate myeloid lineage. Floating cells usually appear six days into the differentiation process. These cells were collected by centrifugation (270*g*, 5 mins, room temperature) and plated back to the same wells with fresh medium. From day 15 to day 26, the medium was switched to SF-Diff medium supplemented with CSF-1 (50 ng ml^{-1}), which was used to generate macrophages from the myeloid progenitors. Cells were cultured in a hypoxia incubator (5% CO_2 and 5% O_2) for the first eight days before being moved to a conventional 5% CO_2 in air tissue culture incubator.

Generation of brain organoids

Brain organoids were generated as described in ref. 7. In brief, human iPS cells were dissociated into single cells using Stempro accutase (Thermo Fisher, catalogue no. A1110501). Nine thousand iPS cells per organoid were then seeded into each well of ultra-low attachment 96-well plates (Corning, catalogue no. CLS3474) in hESC medium supplemented with rock inhibitor (50 µM) and FGF2 (4 ng ml^{-1}) to promote embryoid body formation. On day 6, the embryoid bodies were transferred to ultra-low attachment 24-well plates (Corning, catalogue no. CLS3473) containing neural induction medium to promote neuro-ectoderm formation. On day 11, the embryoid bodies were embedded into Matrigel (Corning, catalogue no. 356234) and transferred to 10 cm dishes (Corning, catalogue no. 430167) containing cerebral organoid medium (B-27 supplement medium without vitamin A) to promote neuroepithelium formation. On day 15, the medium was switched to cerebral organoid medium (B-27 supplement medium with vitamin A) and the organoids were placed on a shaker (Stuart, orbital shaker, SSL1) at 85 rpm to maximize nutrient absorption and allow for the further maturation of each organoid. The medium was changed every three days to allow for optimal availability of nutrients and maturation of the organoids and ensure their long-term survival. The number of organoid/batches used for each iPS cell in this study is described Supplementary Table 4.

Generation of microglia-sufficient brain organoids

One hundred and fifty thousand iMac (day 26) were cocultured with one organoid (day 26) in 1 ml of cerebral organoid medium (containing B-27 supplement medium with vitamin A, and 100 ng ml^{-1} CSF-1) in ultra-low attachment 24-well plates (Corning, catalogue no. 3473) to reduce the adhesion of iMac. This time point is referred to as day 0 and taken as a reference for all subsequent experiments in this study. On day 2, another 1 ml of cerebral organoid medium (containing B-27 supplement medium with vitamin A, and 100 ng ml^{-1} CSF-1) was added into each well. From day 5, half of the medium was changed every three days for a further 18 days unless otherwise stated. The number of organoid/batches used for each iPS cell in this study is described Supplementary Table 4.

Differentiation of cortical neurons from human iPS cells

A protocol of differentiation of cortical neurons described previously[64] was used with a modification. In brief, control iPS cell colonies were maintained on Matrigel-coated six-well plates in mTeSR1 medium. When the confluence of the cells reached 95% or more, the medium was changed to neural induction medium consisting of a 1:1 mixture of DMEM/F-12 (Gibco) and Neurobasal (Gibco) medium supplemented with 0.5× N2 supplement, 0.5× B-27 supplement, 5 μg ml^{-1} insulin (Sigma-Aldrich), 2 mM L-Glutamine, 0.5× MEM-NEAA, 100 μM β2-mercaptoethanol, 0.5× penicillin/streptomycin, 500 ng ml^{-1} mouse Noggin-CF chimera (R&D systems) and 10 μg ml^{-1} insulin, 2 mM L-Glutamine, 0.5× MEM-NEAA, 100 μM β2-mercaptoethanol and 0.5× penicillin/streptomycin. The medium was changed every other day for eight days. NPCs were dissociated using StemPro Accutase (Gibco) and re-plated on poly-L-ornithine (PLO) (Sigma-Aldrich) and laminin-coated six-well plates in neural maintenance medium. Half of the medium was changed every other day for ten days. Neurons were dissociated using StemPro Accutase and re-plated on PLO and laminin-coated six-well plates in neural maintenance medium. Half of the medium was changed every three days for 30 days.

Coculture iMac with cortical neurons in 2D

After treatment of StemPro Accutase, 200,000 hiMac were seeded on cortical neurons on six-well plates. Cells were cultured in neural maintenance medium with 50 ng ml^{-1} of CSF-1. Half of the medium was changed every three days until use.

Bulk RNA sequencing and transcriptome quantification in 2D co-iMac

After 14 days of coculture, cells were washed with phosphate-buffered saline (PBS). Cells were dissociated using StemPro Accutase for 5 min in a CO_2 incubator. After neutralization with FACS buffer, cells were spun down and resuspended in a huma-blocking buffer. Cells were stained with FITC anti-human CD14 (HCD14, BioLegend, catalogue no. 325604), Alexa Fluor 700 anti-human CD11b (ICRF44, BD Biosciences, catalogue no. 557918), PE anti-human CD44 (515, BD Biosciences, catalogue no. 550989), PE anti-human CD184 (12G5, BD Biosciences, catalogue no. 555974), PE-Cy7 anti-human CD24 (ML5, BD Biosciences, catalogue no. 561646) and V450 anti-human CD15 (HI98, BD Biosciences, catalogue no. 561584) for 20 min at 4 °C. After washing cells with FACS buffer, cells were resuspended in FACS buffer with DAPI. Cells were sorted using BD FACSAria II Cell Sorter (BD Biosciences). Total RNA was extracted using an Arcturus PicoPure RNA Isolation kit (Applied Biosystems) according to the manufacturer's instruction. All RNAs were analysed on Agilent Bioanalyser for quality assessment. cDNA libraries were prepared using 2 ng total of RNA and 1 μl of a 1:50,000 dilution of ERCC RNA Spike in Controls (Ambion) using the SMARTSeq v2 protocol[65] with the following modifications: (1) use of 20 μM TSO and (2) use of 250 pg of cDNA with 1/5 reaction of a Nextera XT kit (Illumina). The length distribution of the cDNA libraries was monitored using a DNA High Sensitivity Reagent Kit (Perkin Elmer) on the Labchip GX system (Perkin Elmer). All samples were subjected to an indexed PE sequencing run of 2 × 51 cycles on HiSeq 2000 (Illumina) at 16 samples per lane.

FASTQ files from the RNA-seq experiment were mapped to the Genome Research Consortium human build 38 using STAR aligner and with GENCODE v.26 annotation. FeatureCounts was used to summarize mapped reads to the gene level. The $\log_2$ reads per kilobase per million mapped reads (RPKM) values were obtained from the gene counts using the EdgeR package running in R. DEG analysis was performed using Limma after normalizing $\log_2$ RPKM with Combat for batch effect correction.

Cryo-sectioning

Brain organoids and portions of mouse and human brains were washed five times in PBS and fixed in 4% PFA for 15 mins (for organoids) or overnight (for mouse, macaque or human brain) at 4 °C. Organoids/tissues were then washed with PBS three times and left in 30% sucrose overnight at 4 °C before being embedded in a 7.5% gelatin/10% sucrose solution at room temperature and finally being moved at 4 °C to allow for the polymerization of the gelatin/sucrose solution. Small blocks containing organoids/tissues were cut out using a scalpel blade followed by snap freezing in dry ice-containing isopentane for storage at −80 °C. The blocks were cut into 20-μm-thick slices using a cryostat (Leica) and the sections were placed onto polysine-coated slides (Thermo Fisher) for immunolabelling.

Immunofluorescence

Brain or organoid sections on polysine-coated slides were blocked with blocking buffer (0.5% Triton X-100, 1% donkey serum in PBS) for 1 h at room temperature. After blocking, the sections were washed three times in PBS before they were labelled with the specified primary antibodies (in PBS containing 1% donkey serum) for 1 h at room temperature. The sections were then washed three times with PBS and labelled with secondary antibodies and DAPI (Thermo Fisher, catalogue no. 62248) (reconstituted in PBS containing 1% donkey serum in PBS) before being embedded in mounting medium (Abcam, catalogue no. ab128982) for further analysis by imaging confocal microscopy. For lipid droplet staining, sections were stained with LipidSpot 610 (Biotum, catalogue no. 70069) (1:1,000 in PBS) for 20 mins at room temperature shortly after the secondary antibody incubations. Images were captured with a confocal laser scanning microscope, FV1000 or FV3000 (Olympus) and analysed with the Imaris Imaging software (Bitplane).

For staining of E14.5 mouse fetal brain presented in Extended Data Fig. 10b, freshly dissected brains were postfixed in 4% PFA overnight. Then, brains were washed three times in PBS before inclusion in standard agarose 3.5% (Eurobio). Brains were sliced on the vibratome (Leica VT1000S) in coronal flat sections. The thickness of the slices was 80 μm for E14.5 brains. Slices were incubated for 1 h at room temperature in blocking buffer containing 0.5% Triton-X100, 1% donkey serum in PBS1X. Slices were washed three times in PBS before incubation in a primary antibody solution (1% donkey serum in PBS) for 2 h at room temperature. Primary antibodies used were Iba1 chicken (1/500, Synaptic System) and Plin2 (1/100, Proteintech). Then, slices were washed three times in PBS before incubation in a secondary antibody solution (1% donkey serum in PBS) for 1 h at room temperature. Secondary antibodies used (1/400, Jackson ImmunoResearch Laboratories) were Alexa Fluor 488-conjugated donkey anti-chicken and Cy3-conjugated donkey serum anti-rabbit. Hoechst was used as a nuclear counterstaining. Slices were washed three time before mounting in Vectashield (Vector Laboratories, Eurobio).

Three-dimensional imaging of brain organoids

Organoids were washed with PBS five times and incubated in 4% PFA for 1 h at room temperature. Organoids were then washed twice in PBS (1 h each), before being sequentially washed in 50% (MetOH/PBS), 70% (MetOH/PBS), 95% (MetOH/PBS), 100% (MetOH), 80% (MetOH/DMSO), 70% (MetOH/PBS) and 50% (MetOH/PBS); each step being carried out for 20 mins at room temperature. Organoids were kept overnight in PBS at 4 °C and then incubated in PBS containing 5% BSA, 2.5% DS, 20% DMSO and 0.3% Triton-X 100 for 5 h at 37 °C. The organoids were then washed three times with PBS (30 mins for each wash) before incubation with primary antibodies for three days at 37 °C in PBS containing 1% BSA, 2.5% DS, 5% DMSO, and 0.3% Triton-X 100. After three days, primary antibodies were removed; organoids were washed three times (for 30 mins each) in PBS containing 3% NaCl, and 0.3% Triton-X 100, and subsequently washed twice with PBS alone (30 mins each). Secondary antibody labelling was carried out in PBS containing 1% BSA, 2.5% DS, 5% DMSO, 0.3% Triton-X 100 for three days at 37 °C. After three days, the secondary antibody mixture was removed and organoids were washed

with PBS containing 3% NaCl and 0.3% Triton-X 100 three times (30 mins each) and subsequently with PBS alone twice (30 mins each). Organoids were stored in PBS overnight at 4 °C before they were embedded in a 2% agarose-in-water gel. Organoids were then washed sequentially in 50% (MetOH/PBS), 70% (MetOH/PBS), 95% (MetOH/PBS), and 100% (MetOH) three times, then 50% benzyl alcohol/benzyl benzoate (BABB) in DMSO and finally in 100% BABB. Each wash was done for 20 mins. The organoids were then imaged using the light sheet Ultramicroscope (LaVision BioTec GmbH, Bielefeld) in BABB with a ×2 objective, numerical aperture 0.5, with a zoom set at 3.2. Images of 569 Z-slices, of 2 µm step size were collected and used to image the whole of the organoid.

For Extended Data Fig. 7c (representative of three stainings) and Extended Data Fig. 6e (representative of three separate staining for each type of organoids), the following protocol was used: day 15 organoids and coculture organoids ($n = 4$ each were fixed in 4% PFA at 4 °C for 6 h and, after several washes in PBS, immunohistochemistry was performed on whole organoids. Organoids were blocked overnight at 4 °C with PBS containing 0.2% gelatin and 4% TritonX-100, and then incubated for 24 h at 4 °C with primary antibodies. Organoids were then rinsed twice in PBS containing 0.1% TritonX-100, followed by several PBS washes, before overnight incubation with secondary antibodies at 4 °C (1/400 in PBS). Hoechst was used for fluorescent nuclear counterstaining. Images were acquired with the Leica TCS SP8 confocal microscope at ×10. ImageJ was used for image processing.

Imaris analysis of colocalization

The spot was created to locate the iMac ($IBA1^+$) in the organoids and the surface was created for $Ki67^+$ NPCs. 'Find spots close to surface' option was used to obtain the number of iMac that are/are not in close proximity to $Ki67^+$ NPCs in the organoids ($n = 3$). The same analysis was done to obtain the number of iMac that are/are not in close proximity to $TUJ1^+$ axons in the organoids ($n = 3$). Image analysis and quantification were performed using the Imaris Imaging software (×64, v.9.3.0).

Acquisition and 3D reconstruction

Organoids were imaged with confocal microscope (Leica TCS Sp8). Images were acquired with a ×10, ×20 and ×40 objectives. Then 3D reconstructions were performed on Imaris Imaging software using the Section tool for colocalization and the Surface tool for reconstruction.

Generation of EGFP-expressing iPS cells

HEK293T cells were grown in DMEM supplemented with 10% fetal calf serum (FCS) with 1% penicillin/streptomycin and maintained in a tissue culture incubator. After reaching about 60% confluence, cells were transfected with plasmids for the generation of third generation Lentiviral particles (pMD2.G (Addgene, catalogue no. 12259, pCMV delta R8.2 (Addgene, catalogue no. 12263)) and CSII-EF1α-enhanced green fluorescent protein (EGFP) (RIKEN, catalogue no. RDB12868) plasmids using Lipofectamine 2000 (Thermo Fisher, catalogue no. 11668019). After 48 h of transfection, the cell culture medium was collected in Amicon Ultra-15 Centrifugal Filter Unit (Merck, catalogue no. UFC901024) and centrifuged at 4,000*g* for 30 mins at 4 °C. Human iPS cells were cultured in mTeSR1 medium supplemented with lentiviruses and 4 µg ml^{-1} polybrene (Sigma-Aldrich, catalogue no. H9268-5G) for 2 h. Cells were cultured in mTeSR1 medium. After four days of viral transduction, single-cell human iPS cell clones were picked up and cultured on Matrigel-coated cell culture plates. The expression level of EGFP was confirmed using flow cytometry. EGFP-expressing human iPS cells were used in further experiments where stated.

Laser ablation

Organoids were cocultured with EGFP-expressing iMac for two weeks and then transferred to Iwaki plates (Iwaki, catalogue no. 3911-035) and Matrigel (Corning, catalogue no. 356237). The movement of macrophages on organoids was visualized using a LaVision TriM Scope II microscope (LaVision BioTec), with a water dipping objective lens (×20 magnification, 1.0 numerical aperture, 2 mmWD; XLUMPLFLN20×W, Olympus) and a Chameleon-pulsed infrared laser (titanium sapphire; Coherent). In brief, a 20 µm × 20 µm square area of the organoid was exposed to a laser (850 nm wavelength) for 30 s. Image acquisition was then performed with approximately 40 stacks with a step size of 2 µm. To generate the time-lapse videos, z-stacks were imaged repeatedly for 2 h, at 1 min intervals. Image analysis was performed using the Imaris Imaging software.

Phagocytosis assay

Organoids were cocultured with EGFP-expressing iMac for two weeks then incubated with amyloid beta (1–42) peptides conjugated to Fluo-555 (Anaspec, catalogue no. AS-60480-01) for 48 h. Organoids were then transferred to Iwaki plates (Iwaki, catalogue no. 3911-035) with Matrigel (Corning, catalogue no. 356237) for stabilization. Live images were acquired using a confocal laser scanning microscope FV1000 (Olympus). Image analysis and quantification were performed using the Imaris Imaging software.

Measurement of brain organoid size

The images of the organoids grown in the presence and absence of iMac were captured daily alongside a scale bar by bright field microscopy. ImageJ software (National Institute of Health) was used to draw the circumference of the organoids. Based on the length of the scale bar, ImageJ software calculated the circumference and cross-sectional area of each organoid.

Whole-cell patch recording in organoids

Whole-cell patch measurements were done as previously described[66,67]. To mark the principal neurons for electrophysiological analysis, organoid samples were infected with pAAV-CaMKIIa-EGFP (Addgene, catalogue no. 50469) at about day 90 of culture. The infected samples were cultured for an additional 30 to 45 days before use. Organoids were transferred to a recording chamber filled with standard artificial cerebrospinal fluid containing the following: 124 mM NaCl, 2.5 mM KCl, 1 mM $MgSO_4$, 2 mM $CaCl_2$, 1.2 mM NaH_2PO_4, 24 mM $NaHCO_3$, 5 mM HEPES and 13 mM glucose, pH 7.3, 310 mOsm (310 mOsm, pH 7.4). Cells were visualized using an optiMOS scientific CMOS camera (qImaging) and monitor. Recording pipettes were pulled with P-1000 (Sutter Instrument Co.). Patch pipettes (4–7 MΩ) were filled with an internal solution containing the following: 130 mM K-Gluconate, 11 mM KCl, 10 mM HEPES, 5 mM NaCl, 5 mM Na-phosphocreatine, 2 mM Mg-ATP, 1 mM $MgCl_2$, 0.3 mM Na-GTP and 0.1 mM EGTA (pH 7.3, 300 mOsm). Access resistance, membrane resistance and membrane capacitance were monitored during the experiment to ensure the stability and the health of cells. Responses of neurons were recorded at a holding potential of −70 mV with the MultiClamp 700B amplifier, Axon Digidata 1550B acquisition system and Clampfit 11.1 (Molecular Devices). Data were analysed using AxoGraph v.1.7.0 (AxoGraph Company) and ported to Prism (GraphPad software) for statistical analysis.

Digestion of brain organoids

Brain organoids were washed five times in PBS and incubated in digestion buffer containing Stempro Accutase, Collagenase (Merck, catalogue no. C5138) and dNase (Merck, catalogue no. 10104159001) for 30 min at 37 °C. The organoids were then gently pipetted up and down ten times using a 1 ml pipette tip to release the cells from the organoids. The remaining cells were released from organoids by agitation at 1,400 rpm on an Eppendorf Thermomixer C, at 37 °C for 10 mins before gently pipetting up and down ten times using a 1 ml tip. Once the cell debris had settled at the bottom of the tube, the supernatant was gently collected and filtered through 70 µm filter paper. The cell suspension was then washed in FACS buffer, centrifuged and the cell pellet collected for downstream analysis.

Conditioned medium experiment, effect on iMac activation

Organoids from KYOU1 human iPS cells on day 23 of differentiation were transferred to a 24-well plate. Organoids were cultured in 1 ml of cerebral organoid medium (containing B-27 supplement medium with vitamin A) for three days. The supernatant was collected and cell debris were removed by centrifugation at 1,200 rpm for 5 min before use as a conditioned medium. iMac from KYOU1 human iPS cells on day 26 of differentiation were harvested and 100,000 iMac were seeded on a 24-well plate in SF-DIFF differentiation medium supplemented with 50 ng ml^{-1} CSF-1 (M-CSF). The next day, the medium was changed to a fresh SF-DIFF differentiation medium, fresh cerebral organoid medium, fresh cerebral organoid medium supplemented with 100 ng ml^{-1} LPS (Sigma-Aldrich) or condition medium. After one day (24 h), iMac were detached from the plate using Stem cell Accutase for 5 min. Cells were spun down and resuspended in human blocking buffer (1% mouse serum (Sigma-Aldrich), 1% rat serum (Sigma-Aldrich) and 2.5% human serum (Gemini Bio products)) in FACS buffer. Where specified, cells were stained by flow cytometry for human CD45, CD14, CD11b, CX3CR1, CD68, CD80, CD86 and HLA-DR.

Neural rosettes development

iMac were cocultured with organoids (150,000 iMac per organoid) in 1 ml of cerebral organoid medium (containing B-27 supplement medium with vitamin A, and 100 ng ml^{-1} CSF-1) in ultra-low attachment 24-well plates (Corning, catalogue no. 3473). On day 2, another 1 ml of cerebral organoid medium (containing B-27 supplement medium with vitamin A, and 100 ng ml^{-1} CSF-1) was added into each well. From day 5, half of the medium was changed every three days for a further 10 days. At day 15, brain organoids were washed five times in PBS and fixed in 4% PFA for 2 h (for organoids) at room temperature. Organoids were washed five times in PBS, then were kept in PBS at 4 °C. The experiment was repeated four times with three organoids per control and experimental sets. For the immunohistochemical staining of neural rosettes, 3 µm sections were stained with SOX2 (Abcam, catalogue no. ab97959) (1:1000 in PBS) for 30 mins at room temperature, and Ki67 (DAKO, catalogue no. M7240) (1:1000 in PBS) for 30 mins at room temperature. Images were captured with an EVOS M5000 microscope (Thermo Fisher Scientific, catalogue no. AMF5000). The absolute number of neural rosettes was manually counted. The EVOS M5000 software was used to draw the perimeter of the organoids and of each neural rosette (external perimeter and lumen perimeter). Based on these parameters, the EVOS M5000 software calculated the areas of the organoids and of each neural rosette ('external area' and 'internal area', μm^2). The density of each neural rosette was calculated as a ratio between the external or internal rosette area and the organoid area ('external density' and 'internal density'). The absolute number of rosettes, their external and internal areas, and their external and internal densities, pooled for each condition among batches, were compared in the presence or absence of iMac using Prism (GraphPad).

EdU proliferation assay

Cell proliferation assay was performed using Click-iT Plus EdU Alexa Fluor 488 Flow Cytometry Assay kit (Thermo Fisher Scientific, catalogue no. C10632) according to manufacturer's instructions. In brief, at day 14 of coculture, organoids and cocultured organoids were treated with 20 µM EdU for 2 h. Organoids were digested using Stem cell Accutase for 15 min. After washing and centrifugation, cells were stained with antibodies specific for cell surface markers at 4 °C for 20 min. After washing in FACS buffer (0.2 µm filtered PBS and 5% BSA), cells were stained with LIVE/DEAD Fixable Blue Dead Cell Stain kit for ultraviolet excitation (Thermo Fisher Scientific, catalogue no. L23105) at 4 °C for 30 min. Cells were washed again in FACS buffer. Cells were resuspended in Click-iT fixative and incubated at room temperature for 15 min. After a washing step in FACS buffer, cells were permeabilized using 1x Click-iT permeabilization and reagent washed at room temperature for 15 min. Click-iT plus reaction cocktail was added to the tube and cells were incubated at room temperature for 30 min. After washing with 1x Click-iT permeabilization and wash reagent, cells were stained for human CD45, CD14, CD11b and CX3CR1 and further analysed on an LSRII flow cytometer. Data were analysed using the FlowJo Software (Tree Star).

Supernatant organoid culture

Cerebral organoids generated from ACS-1023 iPS cells were cultured (one per 24-well plate) from day 26 in 2 ml cerebral organoid medium (derived from microglia-sufficient coculture brain organoid well after two days, containing B-27 supplement medium with vitamin A, and 100 ng ml^{-1} CSF-1). The organoid was cultured for the next 28 days with half of the medium changed after every two days for optimal growth of organoid by ensuring maximal nutrient absorption. The experiment was repeated three times with at least four organoids per control and experimental sets.

Organoid coculture with ABCA1 inhibitor-Probucol

Probucol experiments were performed as previously described[48,49]. Cerebral organoid cocultures (from ACS-1023 iPS cells) with 150,000 iMac per organoid (day 26) in 24-well plates started with 1 ml of cerebral organoid medium (containing B-27 supplement medium with vitamin A, 100 ng ml^{-1} CSF-1 and 1 µM Probucol). Then, 1 ml of cerebral organoid medium (containing B-27 supplement medium with vitamin A, 100 ng ml^{-1} CSF-1 and 1 µM Probucol) was added per well on day 2. From day 5 onwards, half of the medium (containing B-27 supplement medium with vitamin A, 100 ng ml^{-1} CSF-1 and 1 µM Probucol) was changed every three days.

Flow cytometry

Digested cells were incubated in blocking buffer (PBS containing 5% FCS) containing the specified antibodies for 30 min at 4 °C. Cells were then incubated with DAPI for nuclear staining and analysed on a BD FACSARIA II/III or BD LSRII (BD Bioscience) for data recording and sorting. For intracellular neutral-lipid staining, digested cells were incubated with with 2 µM 4,4-difluoro-1,3,5,7,8-pentamethyl-4-bora-3a,4a-diaza-s-indacene ($BODIPY^{493/503}$, Thermo Fisher, catalogue no. D3922) in PBS for 20 mins at 37 °C. The cells were then washed with PBS three times before being further incubated with the specified antibodies as mentioned above. Data were analysed on FlowJo (Tree Star).

Real-time quantitative PCR

Real-time quantitative polymerase chain reaction (RT-qPCR) was performed as described in ref. 68. Using an BD FACSARIA II/III (BD Bioscience), 500 iMac or co-iMac (iMicro) were sorted in lysis buffer to extract RNA from the cells. The reverse transcription reaction was carried out in SuperScript IV VILO Master Mix (Thermo Fisher, catalogue no. 11766050) to obtain cDNA. The fluorescence from the Gotaq qPCR Master Mix (Promega, catalogue no. A6002) was detected using LightCycler 480 Real-Time PCR system (Roche). Expression levels of P2RY12, *TMEM119*, *CX3CR1* and *SALL1* were normalized to that of *HPRT1*. Primer pairs used were as follows: P2RY12 forward: 5′-GATGCCACTCTGCAGGTTG-3′, reverse: 5′-GTGCACAGACTGGTGTTACC-3′; *TMEM119* forward: 5′-CACGGACTCTCTCTTCCAG-3′, reverse: 5′-GCAGCAACAGAAGGATGAGG-3′; *SALL1* forward: 5′-ACCTTCTCCTCATCGAGTGC-3′, reverse: 5′-GCTATTCCACATGTGAGTGCC-3′; CX3CR1 forward: 5′-CTTACGATGGCACCCAGTGA-3′, reverse: 5′-CAAGGCAGTCCAGGAGAGTT-3′; *HPRT1* forward: 5′-TGACCAGTCAACAGGGGAC-3′, reverse: 5′-TGCCTGACCAAGGAAAGC-3′. From the low expression level, *SALL1* qPCR was used for 50 cycles instead of 40 cycles for P2RY12, *TMEM119* and *CX3CR1*.

Axon measurement

Organoids cultured either in the presence or absence of iMac for 18 days were digested into single cells and NPCs were sorted using an BD FACSARIA II/III (BD Bioscience). Then, 150,000 FACS-sorted NPCs were seeded onto Poly-L-ornithine (Sigma-Aldrich, catalogue no. P4957) and Laminin (Gibco, catalogue no. 23017-015) coated cover glasses in cerebral organoid medium (containing B-27 supplement medium with vitamin A and 50 μM rock inhibitor). After 48 h the cells were labelled with anti-human TUJ1 antibody and stained with DAPI. The number and length of axons was measured for each cell using Imaris Imaging software.

Cholesterol transportation

iMac (day 26) were cultured in cerebral organoid medium containing 100 ng ml^{-1} CSF-1 and 2 μM cholesteryl 4,4-difluoro-5,7-dimethyl-4-bora-3a,4a-diaza-s-indacene-3-dodecanoate (Thermo Fisher, catalogue no. C3927MP, herein labelled BODIPY^{CE}) overnight. iMac were then washed three times in PBS before being analysed by flow cytometry and immunohistochemistry to confirm successful labelling. Once confirmed, labelled iMac were cocultured with organoids for seven days in cerebral organoid medium containing 100 ng ml^{-1} CSF-1.

Cholesterol transfer using transwell assay

Each organoid was placed in the upper compartment of a transwell plate (Corning, catalogue no. CLS3396) and cultured for seven days in the absence or presence of 150,000 iMac that were prelabelled with 2 μM BODIPY^{CE} and seeded in the lower compartments. The culture was carried out in 1 ml cerebral organoid medium containing 100 ng ml^{-1} CSF-1. On day 3 of the culture, the medium was changed to 1 ml cerebral organoid medium containing 100 ng ml^{-1} CSF-1. In the absence of iMac, 2 μM BODIPY^{CE} was directly added into the medium.

Sample preparation for single-cell RNA-seq

Organoids (cultured in the absence or presence of iMac for 18 days) were digested into single cells and washed once in 0.04% BSA supplemented PBS. iMac cultured in the absence of organoids for 18 days were also subjected to the same digestion and washing processes. The cells were then resuspended to a final cell concentration of 530–1,000 cells per μl in PBS/0.04% BSA. Using the 10X Genomics Chromium Controller, about 8,700 cells were encapsulated in droplets at a targeted cell recovery of 5,000 cells, resulting in estimated multiplet rates of 3.9%. Single-cell RNA-seq libraries were prepared using the 10X Genomics Chromium Single Cell 5′ v1 Library & Gel Bead Kit and i7 Multiplex Kit according to the manufacturer's protocol. The libraries were subjected to an indexed paired-end sequencing run of 2 × 151 cycles on an Illumina HiSeq 4000 (Illumina) at a sequencing depth of 50,000 reads per cell.

Single-cell RNA-seq data preprocessing

The cell ranger pipeline (v.2.1.1) was used to preprocess the 10X sequencing data generated by the 10X Genomics Chromium Controller. Illumina BCL files were converted to FASTQ files using the cellranger mkfastq command. Each read from the FASTQ files were then aligned to a human reference genome (GRCh38-1.2.0) using the Cellranger count command to generate count matrix. The output (count matrix) was used as the main input file for all downstream analysis.

Integration of the 10X datasets

Using Seurat R package v.3.2.2 (ref. 69), the two count matrices (organoid only and coculture) were turned into Seurat object format, combined, log-normalized and then passed through the FindIntegrationAnchors function in Seurat to identify the set of anchors (Anchorset) between the two datasets. The Anchorset was then used to integrate the datasets using the IntegrateData function. The output, containing the cell-to-cell distance matrix, was used for linear dimensionality reduction by principal component analysis, followed by application of the nonlinear *t*-distributed stochastic neighbourhood embedding (*t*-SNE) dimensionality reduction method. The cells projected on the *t*-SNE space were annotated using the average expression (gene set score in each cell) of the canonical markers that have been previously described for defining neurons, NPCs, iMac and mesenchymal cells[12,24]. Significantly, DEGs between the cell types of interest were identified using the Wilcoxon rank sum test implemented in the FindMarkers function of Seurat. The adjusted *P* value was calculated by Bonferroni correction based on all tested genes, and only DEGs with adjusted $P < 0.05$ were used for downstream interpretations such as pathway analysis and plot creation. Downloaded data from the human brain atlas and fetal microglia were integrated as previously described. The integrated data was then subjected to UMAP for dimensional reduction[70]. Identity score of iMicro transcriptome compared to microglia transcriptome from the Allen Brain Atlas[39] was done by scoring genes as per the AddModuleScore function in Seurat[69]. In brief, the function calculates the average expression level of each gene input and identifies which cells best represent the combined expression of those genes.

Gene regulatory network analysis

The single-cell transcriptomic data were also used to construct global gene regulatory networks (regulons) using the SCENIC R package (v.1.1.2), as previously described[31]. A regulon refers to a transcription factor and its putative target genes. The output for a SCENIC analysis is a matrix consisting of AUCell scores (regulon activities) in individual cells. The regulon activity matrix was passed through the Seurat pipeline for identifying differentially active regulons between the cell types. Downstream analysis for regulons were performed using the same approach mentioned above for DEGs.

Alignment with human fetal brain gene expression data

The DEG testing was first performed between all coculture and all organoid-only conditions (from current study) using the Wilcoxon rank sum test in Seurat. The expression of all statistically significant genes (from our cell types' DEGs list) was then depicted across 13 time points of fetal brain development (using data from 273 human embryos, provided in the Allen Brain Atlas (http://www.brain-map.org))[70].

Alignment with mouse datasets

Publicly available processed datasets including mouse single-cell RNA-seq data on the mouse cerebral cortex at E14.5 (ref. 51), under accession GSE123335 and mouse microarray data[50], under accession GSE107129, were downloaded from the Gene Expression Omnibus and were used for projecting the curated DEGs list obtained from the current study.

Gene ontology

All DEGs with adjusted $P < 0.05$ were imported into the PANTHER classification system (http://www.pantherdb.org) for gene ontology (GO) analysis according to the developers' instructions[71].

Pathway network analysis

The pathways network to unravel biological and metabolic functions of cells using differentially expressed proteins was established using ClueGO (v.2.5.7), a plug-in application in Cytoscape (v.3.8.0)[72,73]. Marker expression was compared using ontology and pathway databases as follows: GO: BiologicalProcess-EBI-UniProt-GOA-ACAP-ARAP (GO: ImmuneSystemProcess-EBI-UniProt-GOA-ACAP-ARAP; KEGG, Reactome: Pathways and WikiPathways. All ontology and pathways databases used were from versions accessed and updated on 8 May 2020). Only pathways with $P < 0.05$ were considered. Settings were as follows: GO Tree Interval (minimum level of 2) and GO Term/Pathway Selection (2 for each cluster being compared). Pathway enrichment/

depletion analysis was done in a two-sided hypergeometric test and using Bonferroni step down.

HDL isolation by ultracentrifugation

HDL from the plasma of a healthy human donor (positive control) or conditioned medium (cM) of day 18 organoid, coculture organoids or iMac were purified using a stepwise ultracentrifugation within a density of 1.063–1.210 g ml^{-1}. First, three solutions were prepared. Solution A ((ρ: 1.006 g ml^{-1}) containing 11.40 g NaCl and 0.1 g EDTA-2Na in 1 l dH_2O), Solution B ((ρ: 1.182 g ml^{-1}) containing 24.98 g of KBr into Solution A) and Solution C ((ρ: 1.478 g ml^{-1}) containing 78.32 g of KBr into Solution A)) were prepared. Then, 150 µl of Solution A was layered onto the 300 µl of sample (plasma/conditioned medium) to increase density to 1.019 g ml^{-1}. The mixture was subjected to ultracentrifugation at 120,000 rpm for 85 mins at 8 °C. The differences in lipoprotein density allowed for the separation and removal of very low-density lipoproteins (vLDL) present at the topmost layer (150 µl) of the sample column. Next, 150 µl of Solution B was added to increase sample density to 1.063 g ml^{-1} and subjected to ultracentrifugation at 120,000 rpm for 125 mins at 8 °C. Then, 150 µl of low-density lipoprotein present at the topmost layer of the sample column was removed before 150 µl of Solution C was added to increase plasma density to 1.21 g ml^{-1}. The sample mixture was then ultracentrifuged at 120,000 rpm for 210 mins at 8 °C. HDL, at the topmost layer of the plasma column was collected and dialysed against excess PBS twice at 4 °C, for 6 h each time using a 7000 MWCO dialysis bag to remove KBr salts. Alternatively, the samples were desalted using Pierce Polyacrylamide Spin Desalting Columns, 7 K MWCO, 0.7 ml (Thermo Scientific, catalogue no. 89862).

Western blotting

Total protein was extracted from iMac cell lysate using 200 µl of radio immunoprecipitation assay lysis buffer containing protease inhibitor (Roche) and Phosphatase Inhibitor Cocktail complex (Merck). The sample was then centrifuged at 12,000*g* at 4 °C for 5 min, and the supernatant was used for further analysis. cM from day 14 iMac culture, organoid alone or coculture organoids were concentrated using Vivaspin, 5 kDa MWCO. The total protein concentration was determined using BCA protein assays (Thermo Scientific Technologies). Protein samples (40 µg) were separated by 15% SDS–PAGE, then transferred to 0.45 mm polyvinylidene fluoride membranes (Millipore). After blocking with 5% skim milk for 1 h, the membranes were incubated overnight at 4 °C with Recombinant Anti-Apolipoprotein E antibody (no. ab52607, Abcam) and then incubated for 1 h at room temperature with horseradish peroxidase-conjugated corresponding secondary antibodies. The immunoreactive protein bands were visualized using SuperSignal West Pico PLUS Chemiluminescent Substrate (catalogue no. 34580, Thermo Fisher Scientific). ImageJ software (National Institute of Health) was used for gray scan analysis. For quantification, band signals were normalized to the Ponceau S signal of the 40 µg protein loaded in the gel. For gel source data, see Supplementary Fig. 1.

Proteomic analysis

Organoids that were cultured either in the presence or absence of iMac for 18 days were digested and pure populations of NPC, neuron, co-NPC, co-neuron and iMicro sorted using an BD FACSARIA II/III (BD Bioscience). Three independent samples (three cocultured organoids and three organoids) were sorted for proteomic analysis and each sample was run in triplicate. iMac alone that were cultured for 18 days in the absence of organoids were also sorted to obtain homogeneous cell populations. Sorted cell populations were lysed in 50 µl urea lysis buffer (8 M urea/Tris-HCl 50 mM, pH 8), reduced in the presence of Tris(2-carboxyethyl)phosphine 20 mM for 20 min at romm temperature and further alkylated with 55 mM 2-chloroacetamide. Following dilution with 400 µl of 100 mM triethylammonium bicarbonate (pH 8.5; Sigma-Aldrich, catalogue no. T7408), samples were digested with lysyl endopeptidase (LysC, Wako, catalogue no. 129-02541) and trypsin (Promega, catalogue no. V5117) in the ratio 1:50 for 4 h and 18 h respectively. Samples were further acidified with trifluoroacetic acid (TFA Sigma-Aldrich, catalogue no. T6508; 1% v/v), spun down 14,000*g* for 10 mins at room temperature and digested peptides were extracted using Oasis PRiME HLB solid phase extraction plates (Waters, catalogue no. WAT058951). Eluted peptides were vacuum-dried and step-fractionated (high pH mode 10 mM ammonium formate mobile phase) on self-packed tip columns using Dr. Maisch Reprosil C18 10 µm beads (Reposil-Pur Basic C18 10 µm, M. Gmbh no. r10.b9.0025). The fractions were collected at 12.5%, 17.5%, 22.5% and 50% acetonitrile concentrations. Eluted fractions were vacuum dried and washed twice with fraction wash buffer (60% acetonitrile, 0.1% formic acid). Each fraction was separated on a 50 cm × 75 µm ID (internal diameter), PepMap RSLC C18 EASY-Spray column (Thermo Scientific) in a 75 min gradient of solvent A (0.1% formic acid in water) and solvent B (99.9 % acetonitrile, 0.1% formic acid in water) on an EASY-nLC 1000 (Thermo Fisher Scientific), coupled to an Orbitrap Fusion Lumos mass spectrometer (Thermo Fisher Scientific). Mass spectra were acquired in data-dependent acquisition mode with a speed mode of −2.5 s cycle using Orbitrap and ion trap analysers (OT-MS1 (Orbitrap precursor ion), AGC (automatic gain control) target -4×10^5 ions, 60,000 resolutions, IT-MS2 (tandem mass spectrometry, fragmented product ions) rapid mode, CID fragmentation 35%). Peak lists were generated using MaxQuant software v.1.6.7.0. Spectra were searched against the target-decoy Human Uniprot database with the following fixed modifications: Carbamidomethyl (C), and variable modifications: Oxidated (M), Deamidated (NQ) Acetyl (N-terminal protein). A maximum of two missed cleavages was allowed, with a mass tolerance of 4.5 ppm mass deviation (after recalibration) for the OT-MS (Orbitrap mass spectrometry precursor ion) survey scan, and 0.5 Da for IT–MS2 ion fragments. The FDR (false discovery rate) was set to 1%. Label-free quantification (LFQ) was performed. Data were analysed using EdgeR (v.4.2) on R between NPCs and co-NPCs.

Lipidomic analysis

Organoids were cultured either in the presence or absence of iMac for 18 days and culture media collected. Culture medium from iMac alone was also collected. Ammonium formate and 1-butanol were obtained from Sigma-Aldrich; MS-grade acetonitrile, methanol and isopropanol from Fisher Scientific; acylcarnitine 16:0 D3, CE 18:0 D6, Cer d18:0/08:0, Cer d18:1/12:0, Cer m18:1/12:0, cholesterol D7, DG 15:0/15:0, GM3 d18:1/18:0 D3, Hex1Cer d18:1/12:0, Hex2Cer d18:1/12:0, Hex3Cer d18:1/18:0 D3, LPC 13:0, LPE 14:0, PC 13:0/13:0, plasmalogen PC 18:0/18:1 D9, PE 17:0/17:0, plasmalogen PE 18:0/18:1 D9, PG 17:0/17:0, PS 17:0/17:0, PI 12:0/13:0, PS 34:0, SM d18:1/12:0 and TG 12:0/12:0/12:0 from Avanti Polar Lipids. Ultrapure water (18 MΩ cm at 25 °C) was obtained from an Elga LabWater system.

Lipid extraction. Culture medium (300 µl) was mixed with 1,350 µl methyl tert-butyl ether/methanol (7:2) (v/v) containing internal standards. The mixture was vortexed for 2 min, sonicated at 4 °C for 30 min and then centrifuged at 3000*g* at 4 °C for 5 min to facilitate phase separation. The upper organic phase was dried by speedvac and reconstituted in 50 µl butanol/methanol (1:1) (v/v) for liquid chromatography with tandem mass spectrometry (LC–MS/MS) analysis.

LC–MS/MS analysis. Lipidomic analyses were performed based on a modified version of a positive ionization MRM (multiple reaction monitoring) method described previously[74]. The LC–MS/MS analysis was performed on an Agilent UHPLC 1290 liquid chromatography system simultaneously connected to an Agilent QqQ 6495 A mass spectrometer. An Agilent rapid resolution HD Zorbax Eclipse-C18 column (2.1 × 50 mm, 1.8 µm) was used for the RPLC (reversed-phase liquid chromatography) separation. Mobile phases A (60% water and 40% acetonitrile with 10 mmol l^{-1} ammonium formate) and B (10% acetonitrile

and 90% isopropanol with 10 mmol l^{-1} ammonium formate) were used for the chromatographic separation. The following gradient was applied: 0–2 min, 20–60% B; 2–12 min, 60–100% B; 12–14 min, 100% B; 14.01–15.8 min, 20% B. The oven temperature was maintained at 40 °C. Flow rate was set at 0.4 ml min^{-1} and the sample injection volume was 2 µl. The positive ionization spray voltage and nozzle voltage were set at 3,000 V and 1,000 V, respectively. The drying gas and sheath gas temperatures were both maintained at 250 °C. The drying gas and sheath gas flow rates were 14 l min^{-1} and 11 l min^{-1}, respectively. The nebulizer nitrogen gas flow rate was set at 35 psi. The iFunnel high- and low-pressure RFs (retention factors) were 150 V and 60 V, respectively.

Nomenclature of lipid species. Among the 25 classes of lipids detected, we assessed the levels of cholesterol-ester (CE), cholesterol (COH), diacylglycerol (DG) triacylglycerol (TG), phosphatidylcholine (PC), phosphatidylethanolamine (PE), phosphatidylglycerol (PG), phosphatidylinositol (PI) and phosphatidylserine (PS).

Label-free quantitative proteomics of laser-cut neural rosettes

Neural rosettes were microdissected from an FFPE (formalin-fixed, paraffin-embedded) 5-µm-thick section stained by hematoxylin with a PALM type 4 (Zeiss) laser micro-dissector. Three technical replicates were done for each experimental condition (equivalent to 1 mm^2, 40–50 rosettes per replicate). Microdissected neural rosettes were incubated in Tris pH 6.8, Sodium Dodecyl Sulfate 2%, Dithiothreitol 10 mM buffer for 2 h at 95 °C. The steps of sample preparation and protein digestion by the trypsin were performed as previously described[75]. Nano LC–MS/MS analyses were performed using an Ultimate 3000 RSLC Nano-UPHLC system (Thermo Scientific) coupled to a nanospray Orbitrap Fusion Lumos Tribrid Mass Spectrometer (Thermo Fisher Scientific). Each peptide extract was loaded on a 300 µm ID × 5 mm PepMap C18 precolumn (Thermo Scientific) at a flow rate of 10 µl min^{-1}. After a 3 min desalting step, peptides were separated on a 50 cm EASY-Spray column (75 µm ID, 2 µm C18 beads, 100 Å pore size, ES903, Thermo Fisher Scientific) with a 4–40% linear gradient of solvent B (0.1% formic acid in 80% ACN) in 57 min. The separation flow rate was set at 300 nl min^{-1}. The mass spectrometer operated in positive ion mode at a 2.0 kV needle voltage. Data was acquired using Xcalibur 4.4 software in a data-dependent mode. MS scans (m/z 375–1,500) were recorded at a resolution of R = 120,000 (at m/z 200), a standard AGC target and an injection time in automatic mode, followed by a top speed duty cycle of up to 3 s for MS/MS acquisition. Precursor ions (2 to 7 charge states) were isolated in the quadrupole with a mass window of 1.6 Th and fragmented with HCD (higher-energy collisional dissociation) at 28% normalized collision energy. MS/MS data were acquired in the Orbitrap cell with a resolution of R = 30,000 (at m/z 200), a standard AGC target and a maximum injection time in automatic mode. Selected precursors were excluded for 60 s. Protein identification was done in Proteome Discoverer 2.5. Mascot 2.5 algorithm was used for protein identification in batch mode by searching against a UniProt *Homo sapiens* protein database (78,139 entries, release 7 March 2021). Two missed enzyme cleavages were allowed for the trypsin. Mass tolerances in MS and MS/MS were set to 10 ppm and 0.02 Da. Oxidation (M) and acetylation (K) were searched as dynamic modifications and carbamidomethylation (C) as static modification. Raw LC–MS/MS data were imported in Proline Web for feature detection, alignment and quantification[76]. Proteins identification was only accepted with at least two specific peptides with a pretty rank = 1 and with a protein FDR value less than 1.0% calculated using the 'decoy' option in Mascot. Label-free quantification of MS1 level by extracted ion chromatograms was carried out with parameters indicated previously[75]. The normalization was carried out on median of ratios. The inference of missing values was applied with 5% of the background noise. A bilateral heteroscedastic t-test was performed to test for significance of variation in relative protein abundances between experimental conditions.

Statistics

Statistical analysis was performed using GraphPad Prism (v.9.0.2) The number of replicates and tests used are detailed in figure legends for each analysis. P values were determined as follows: $^*P \le 0.05$; $^{**}P \le 0.01$; $^{***}P \le 0.001$; $^{****}P \le 0.0001$. Unless otherwise stated, only P values statistically significant ($P \le 0.05$) are added to the plots.

Ethic approval statement and informed consent

Human fetal tissues (brain) were obtained in accordance with Singapore Sing-Health and National Health Care Group Research Ethics Committees. All women gave written consent to the use of fetal tissues according to internationally recognized guidelines (Polkinghorne, 1989). Review of the guidance on the research use of fetuses and fetal material (CM 762). All fetal tissues were obtained from 2nd trimester (12–22 weeks estimated gestational age) elective pregnancy terminations carried out for sociopsychological reasons. All fetuses were considered structurally normal on ultrasound examination before termination and by gross morphological examination following termination. Fetal tissues from 2nd trimester of gestation were used for this study. Patient-derived iPS cells were generated from three boys (patients 515, 519 and 534) and one girl (patient 523) with H3K27M diffuse midline glioma. This information has been collected from the anonymized case report form filled out by the patient's medical doctor after having obtained patient/family's consent. Study was approved by the Gustave Roussy Ethic Committee. C57BL/6 mice (CD45.1 and CD45.2) were from the Biological Resource Center, Agency for Science, Technology and Research, Singapore. All experiments and procedures were approved by the Institutional Animal Care and Use Committee of the Biological Resource Center (Agency for Science, Technology and Research, Singapore) in accordance with the guidelines of the Agri-Food and Veterinary Authority and the National Advisory Committee for Laboratory Animal Research of Singapore (ICUAC no. 151071).

Reporting summary

Further information on research design is available in the Nature Portfolio Reporting Summary linked to this article.

Data availability

The raw scRNA-seq and bulk-seq sequencing data of this study have been deposited in Gene Expression Ominbus with accession nos. GSE242894 and GSE241127 respectively. Proteomic data on purified cell populations have been deposited on JPOST (JPST001822) and Proteome Exchange (PXD042344). Neural rosette proteomic data are available via ProteomeXchange with identifier PXD044406. All lipidomic data have been deposited in Mendeley Data, which can be accessed at https://doi.org/10.17632/t573dphyc5-1.

Code availability

All codes and software used in this study are listed in the reporting summary and in the Methods section where appropriate. No new software or code was generated and used for data collection and analysis.

64. Shi, Y., Kirwan, P. & Livesey, F. J. Directed differentiation of human pluripotent stem cells to cerebral cortex neurons and neural networks. *Nat. Protoc.* **7**, 1836–1846 (2012).
65. Picelli, S. et al. Full-length RNA-seq from single cells using Smart-seq2. *Nat. Protoc.* **9**, 171–181 (2014).
66. Lopez-Hernandez, G. Y. et al. Electrophysiological properties of basal forebrain cholinergic neurons identified by genetic and optogenetic tagging. *J. Neurochem.* **142**, 103–110 (2017).
67. Trombin, F., Gnatkovsky, V. & de Curtis, M. Changes in action potential features during focal seizure discharges in the entorhinal cortex of the in vitro isolated guinea pig brain. *J. Neurophysiol.* **106**, 1411–1423 (2011).
68. Ho, V. et al. Expression analysis of rare cellular subsets: direct RT-PCR on limited cell numbers obtained by FACS or soft agar assays. *Biotechniques* **54**, 208–212 (2013).

69. Stuart, T. et al. Comprehensive integration of single-cell data. *Cell* **177**, 1888–1902 e21 (2019).
70. Becht E. et al. Dimensionality reduction for visualizing single-cell data using UMAP. *Nat. Biotechnol.* **37**, 38–44 (2019).
71. Mi, H. et al. PANTHER version 16: a revised family classification, tree-based classification tool, enhancer regions and extensive API. *Nucleic Acids Res.* **49**, D394–D403 (2021).
72. Bindea, G., Galon, J. & Mlecnik, B. CluePedia Cytoscape plugin: pathway insights using integrated experimental and in silico data. *Bioinformatics* **29**, 661–663 (2013).
73. Bindea, G. et al. ClueGO: a Cytoscape plug-in to decipher functionally grouped gene ontology and pathway annotation networks. *Bioinformatics* **25**, 1091–1093 (2009).
74. Sieber-Ruckstuhl, N. S. et al. Changes in the canine plasma lipidome after short- and long-term excess glucocorticoid exposure. *Sci. Rep.* **9**, 6015 (2019).
75. Henriet, E. et al. Argininosuccinate synthase 1 (ASS1): a marker of unclassified hepatocellular adenoma and high bleeding risk. *Hepatology* **66**, 2016–2028 (2017).
76. Bouyssie, D. et al. Proline: an efficient and user-friendly software suite for large-scale proteomics. *Bioinformatics* **36**, 3148–3155 (2020).

Acknowledgements We thank all the members of the Ginhoux laboratory for helpful discussions. Flow cytometry and cell sorting, microscopy and RNA library preparation were carried out on SIgN platforms (supported by BMRC IAF311006 grant and BMRC transition funds no. H16/99/b0/011), Agency of Science, Technology and Research (A*STAR), Singapore. F.G. was supported by EMBO YIP, A*STAR UIBR award, Singapore National Research Foundation Senior Investigatorship (NRFI2017-02) and the Fondation Gustave Roussy. R.M.S. was supported by BMRC, A*STAR core funding and Singapore NRF SIS. M.A.P. was supported by the BC Children's Health Research Institute Investigator Grant (IGAP) Award, and a Scholar Award from the Michael Smith Health Research BC. We acknowledge S. Garel for discussion at IBENS, Astou Tangara and the IBENS imaging facility (IMACHEM-IBiSA), member of the French National Research Infrastructure France-BioImaging (ANR-10-INBS-04), with support from the 'Fédération pour la Recherche sur le Cerveau - Rotary International France' (2011) and from the programme « Investissements d'Avenir » ANR-10-LABX-54 MEMOLIFE. N.O. is supported by the Fondation pour la Recherche Médicale (FRM, EQU202003010195). M.S.T. is supported by CNRS and the Fondation pour la Recherche sur le Cerveau (FRC). We thank L. Robinson, Insight Editing London, for editing the manuscript.

Author contributions D.S.P., T.K., M.A.P., O.N.F.C. and F.G. designed experiments and interpretation. D.S.P., J.Z., M.A.P. and F.G. designed the coculture protocol. D.S.P., T.K. and S.K.T. performed functional experiments. D.S.P., O.L., K.H.U., W.T.K., Z.Y.B, N.W.D. and W.J.W. performed iMac and organoid cultures. A.S., C.A.D. and S.A. provided advice and interpretation. D.S.P., A.B., L.T., Y.T. and L.G.N. performed imaging analysis. F.T., A.T., W.K.T., L.G. and M.R.W. performed lipidomic mass spectrometry and data analysis. N.O. and M.S.T. performed microscopy analysis on organoids. C.H.T., V.A., M.C.M., I.B. and B.M. characterized the lipoprotein particles. B.V. and R.T.K. provided the CTRL iPS cell line. M.M., L.G. and C.P. generated the iPS cells from paediatric patients and associated experiments. D.C., J.G. and V.M. provided fibroblasts from paediatric patients. J.K.Y.C. provided the human fetal brain tissues. S.D.T., J.-W.D. and F.S. characterized neural rosettes and performed proteomic analysis. W.W.P. and R.M.S. performed proteomic mass spectrometry analysis on purified cell subsets. A.K., X.M.Z., S.K., J.L., K.D., J.C., S.W.H., G.D. and S.R. performed analysis of RNA-seq data. D.S.P., I.L., Z.M.L., J.M.O. and S.L. performed flow cytometry analysis and sorting. X.Y.Y. and S.Y.J. ran patch-clamp analysis and electrophysiological characterization of brain organoids. D.S.P., O.N.F.C. and F.G. wrote the manuscript. All authors read and agreed with the manuscript.

Competing interests D.S.P., J.Z., M.A.P. and F.G. are inventors in 'Microglia-sufficient brain organoids' Patent Application No: 10201902893S.

Additional information

Supplementary information The online version contains supplementary material available at https://doi.org/10.1038/s41586-023-06713-1.

Correspondence and requests for materials should be addressed to Florent Ginhoux.

Peer review information *Nature* thanks Veronique Miron and the other, anonymous, reviewer(s) for their contributionto the peer review of this work. Peer reviewer reports are available.

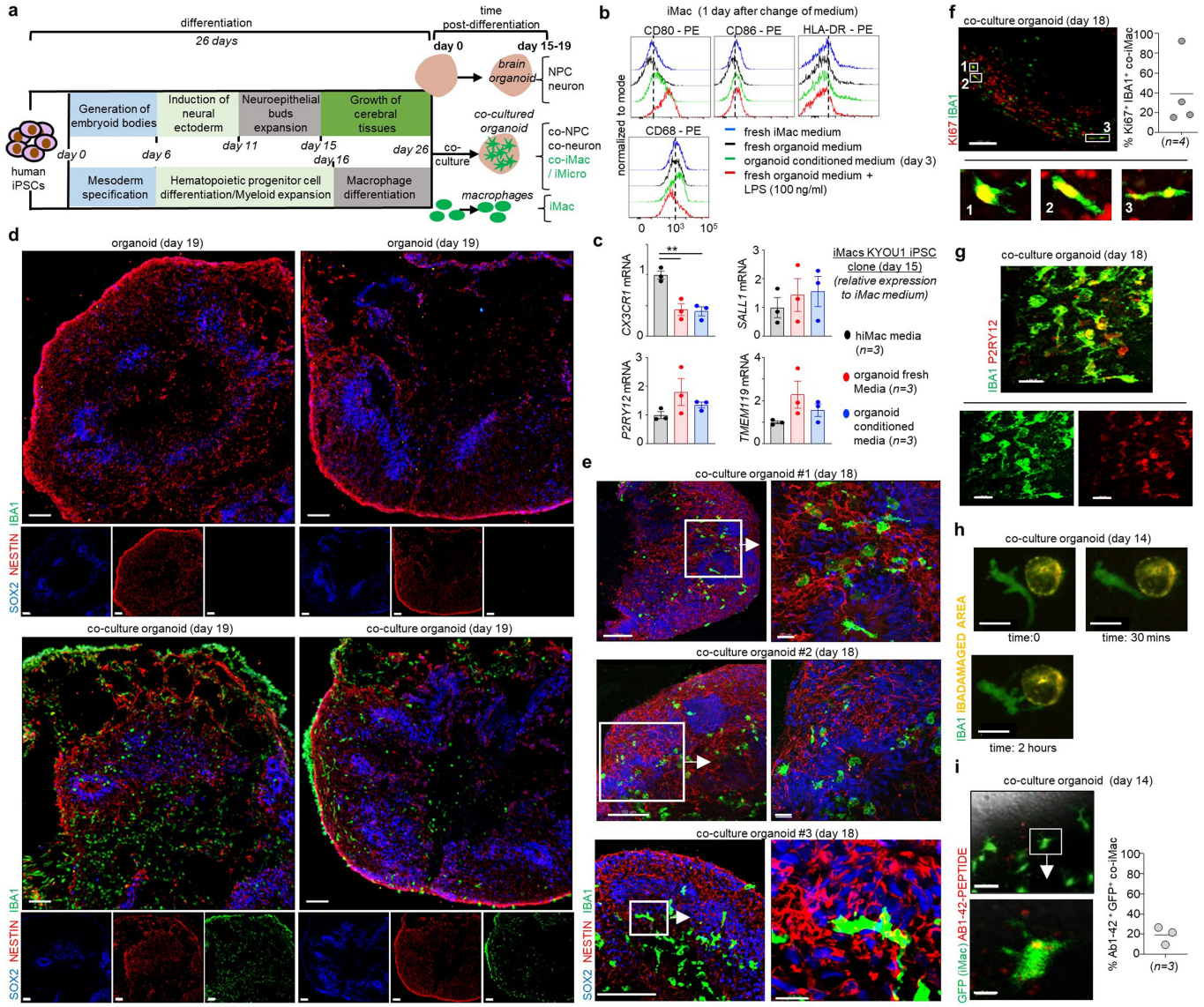

Extended Data Fig. 1 | Phenotypic characterization of iMicro. a, Full Schematic overview of the generation of microglia-sufficient brain organoids. iMac and brain organoid are obtained 26 days after initial iPSC culture and constitute **day 0** iMac and organoids. Co-cultured organoids are analysed from 15 days onwards (day 15) of co-culture of day 0 iMac and organoids. iMac co-cultured with brain organoids are characterised as co-iMac initially and then iMicro. Unless otherwise stated, experiments throughout the study are performed using the KYOU1 iPSC line. **b**, Flow cytometry analysis of activation markers by iMac in various conditions: treated for 24 h with fresh iMac medium, fresh cerebral organoid medium, cerebral organoids conditioned medium, or fresh cerebral organoids medium supplemented with LPS (100 ng/ml) for 24 hrs (representative of n = 3). **c**, RT-qPCR data showing the expression levels of microglia-specific markers in iMac grown for 15 days in iMac medium, fresh cerebral organoid medium and cerebral organoid conditioned medium (n = 3 each). Statistical analysis, one-way ANOVA. Error bars, mean +/− s.e.m. **d**, Sectioning and immunofluorescence analysis of brain organoids co-cultured with (n = 2) or without (n = 2) iMac for 19 days for NESTIN, SOX2 and IBA1. Individual staining profile are shown below each merged staining. Scale bar, 100 µm. **e**, Immunofluorescence staining for SOX2, NESTIN and IBA1 of day 18 co-culture organoids (3 represented from n = 4). *Boxed areas* are shown on the right in higher magnification. Scale bar, 100 µm and 20 µm. **f**, Sectioning and immunofluorescence staining of brain organoids co-cultured with iMac for 18 days showing the positivity of IBA1$^+$ iMac for Ki67. Quantification performed using the Imaris Imaging software. Scale bar, 100 µm (n = 4). **g**, Immunofluorescence staining for expression of P2RY12 by IBA-1$^+$ co-iMac (day 18). Scale bar, 20 µm. Representative of 3 independent staining. **h**, EGFP-expressing iMac elongates its dendrites towards the neuronal injury induced by two-photon laser ablation. Scale bar, 20 µm. (Representative of multiple experiments with same observation). **i**, Live imaging showing EGFP-expressing iMac that actively moved on the organoid and contained Ab1-42 peptide-TAMRA suggesting their ability to survey the organoid and phagocytose the peptides. Scale bar, 50 µm. *Boxed area* highlighted below. Scale bar: 10 µm (n = 3). Quantification performed using the Imaris Imaging software.

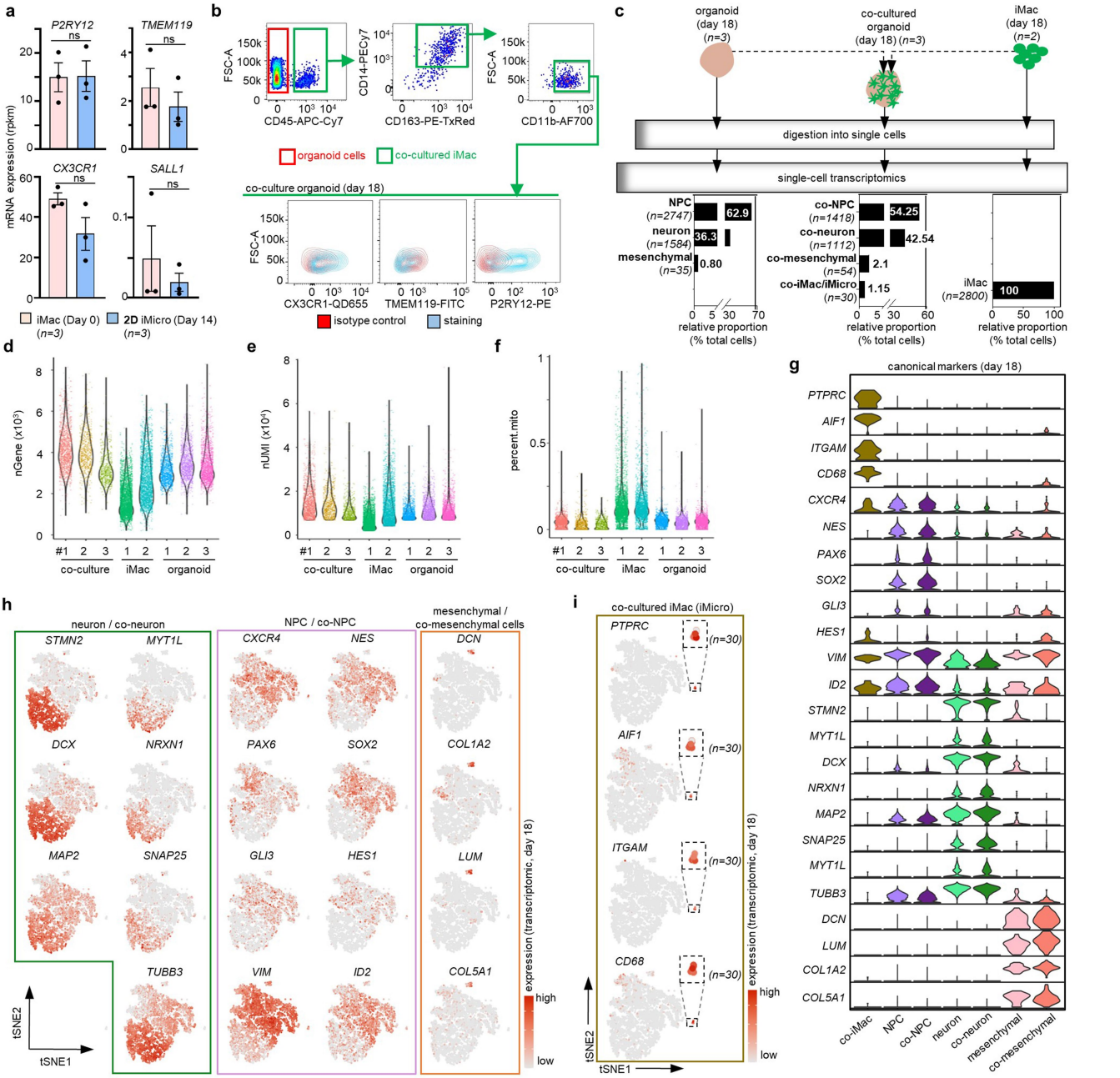

Extended Data Fig. 2 | Identity of cell populations from single-cell RNAseq data. a, Expression of microglia-specific markers *P2RY12*, *SALL1, CX3CR1* or *TMEM119* in iMac alone (n = 3, day 0) and co-iMac co-cultured in 2 dimension (2D) with iPSC-derived cortical neurons supplemented with 50 ng/ml CSF-1 (n = 3, day 14). Data obtained from bulk RNA-seq. Statistical analysis, one-way ANOVA. ns, non-significant. Error bars, mean +/− s.e.m. **b**, Flow cytometry panel and gating strategy used to assess the expression levels of microglia-specific markers in co-iMac. **c**, Schematic overview of the single-cell RNA-seq experimental procedure. Number of cells analysed is shown for purified NPC & neuron (n = 3), co-NPC, & co-neuron (n = 3), iMac (n = 2) and co-cultured iMac (n = 3) obtained at day 18. The relative proportions of each cell type (and associated absolute counts) analysed in each condition are represented. **d**, Violin plot depicting the number of genes detected in each single cell analysis. **e**, Violin plot for nUMI. **f**, Violin plot depicting the percentage of mitochondrial genes. **g**, Violin plots showing the expression level of canonical markers used to define iMac, NPC, neurons and mesenchymal cells isolated from organoids and co-culture organoids. **h**, tSNE plots showing the expression level of canonical markers used to define NPC, neurons and mesenchymal cells. **i**, tSNE plots showing the expression levels of canonical markers used to define iMac (termed co-iMac/iMicro in co-cultured organoids). **d-i**, Data displayed correspond to data analysis from RNA-seq performed on cells obtained from day 18 organoid and co-culture organoids. **h, i**, tSNE plots are of the concatenated data ie. organoid alone and co-culture organoids.

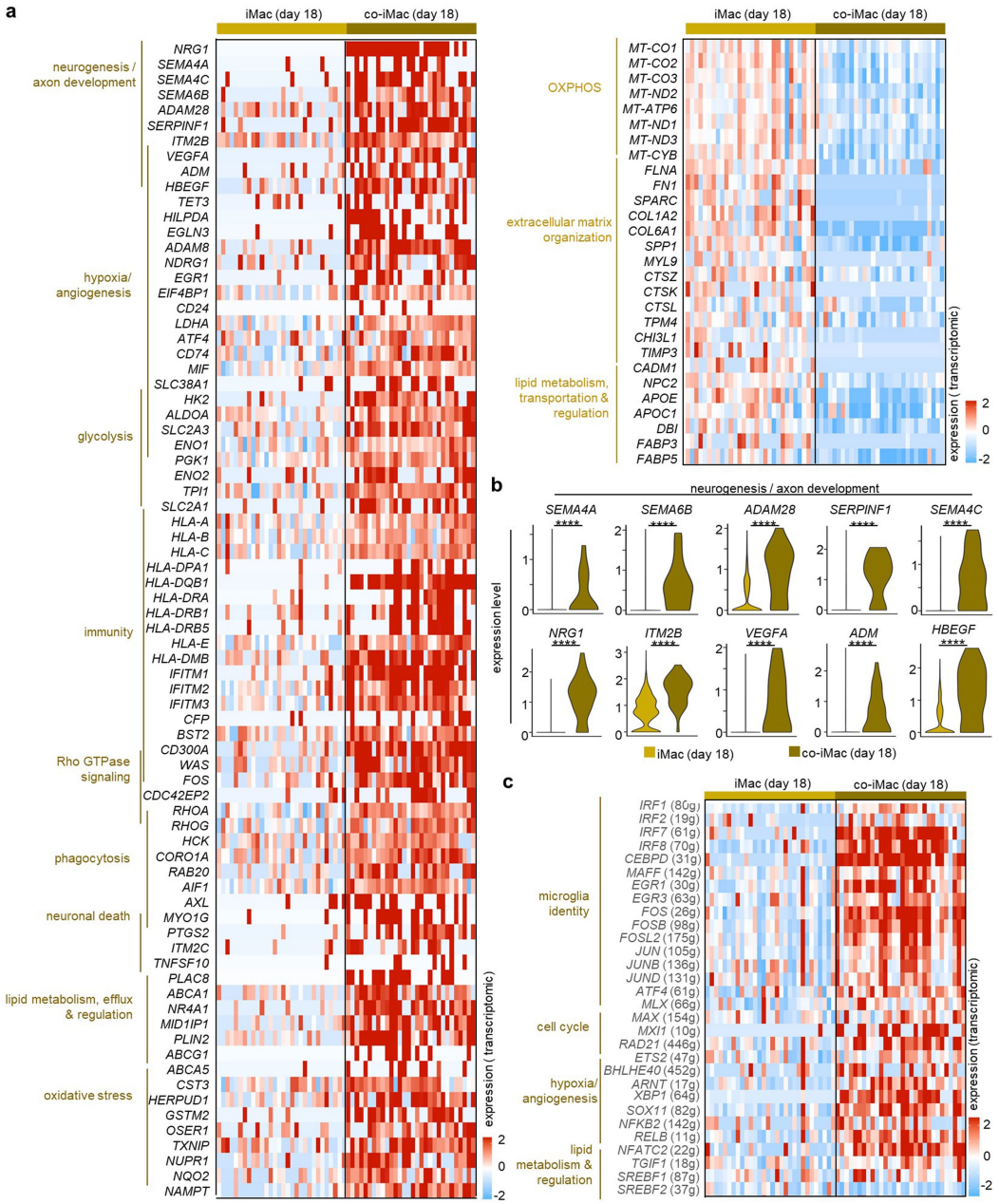

Extended Data Fig. 3 | Transcriptomic signature of iMicro. a, Heatmap showing the expression levels of genes more- or less-highly expressed in iMac in co-culture organoids (co-iMac) at day 18. **b**, Violin plots comparing the expression levels of genes involved in neurogenesis and axon development between day 18 iMac and co-iMac. Statistical analysis, Mann-Whitney test. **c**, Heatmap showing the expression levels of regulons more- or less-highly expressed in day 18 iMac and co-iMac. **a-c**, Data displayed correspond to data analysis from RNA-seq performed on cells obtained at day 18.

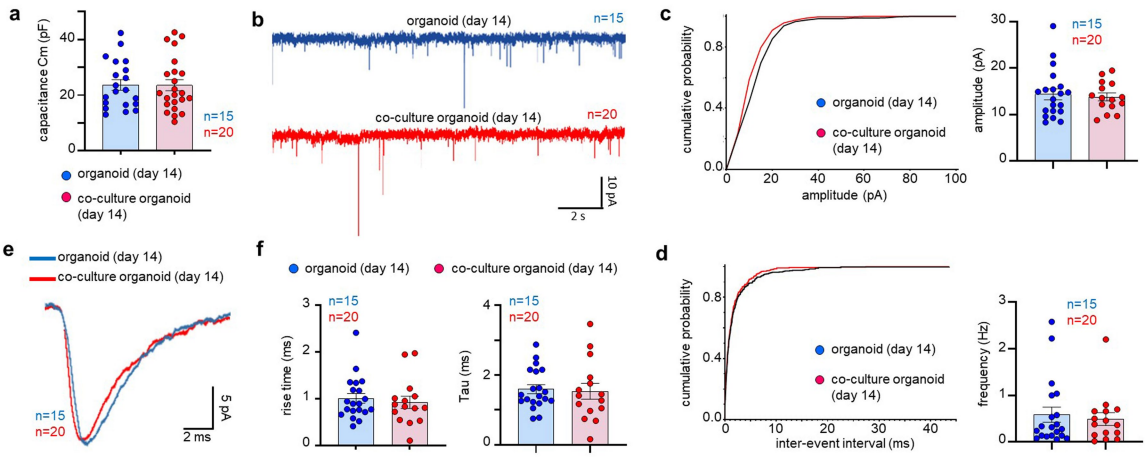

Extended Data Fig. 4 | Electrophysiological profile of co-culture brain organoids. a, Plots representing the capacitance (Cm) of neuronal cells between organoids (n = 15) and co-culture organoids (n = 20) at day 15. **b**, Representative current traces of spontaneous postsynaptic currents (sPSC) obtained from whole cell patch clamp recording of day 15 brain organoids with or without iMac (n = 15, n = 20 respectively). **c, d**, Amplitude and Frequency of neurons from day 15 organoids co-cultured with (n = 15, n = 20 respectively) or without iMac. **e**, Representative traces of individual spontaneous postsynaptic current kinetic responses (sPSC) in day 15 organoid cultures with (n = 20) and without (n = 15) iMac. **f**, Rise and decay time (Tau) of sPSC responses of neurons in the presence (n = 15) or absence (n = 20) of iMac. **a, c, d, f**, Statistical analysis, Mann-Whitney U test. Error bars, mean +/− s.e.m.

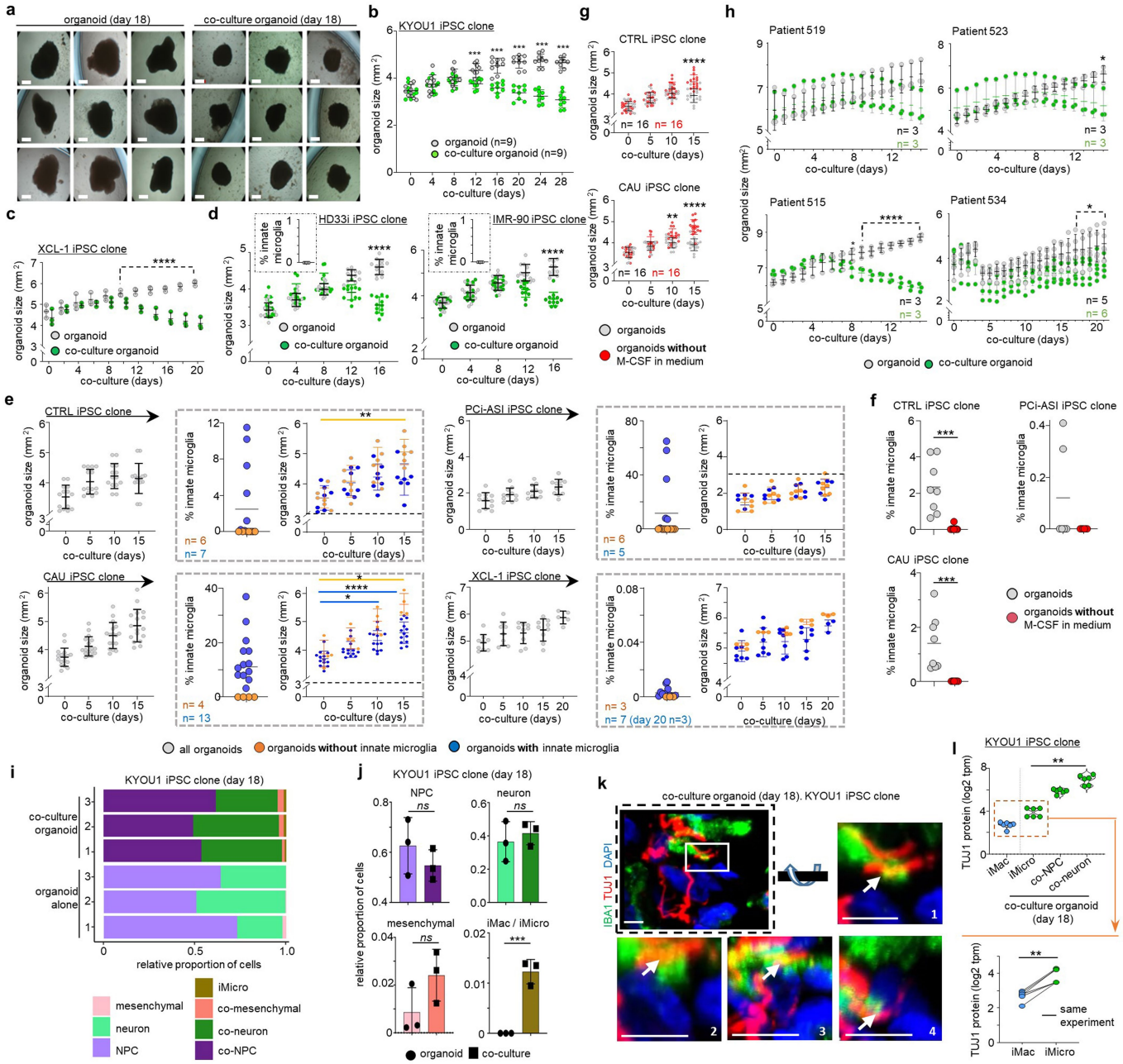

Extended Data Fig. 5 | See next page for caption.

Extended Data Fig. 5 | Generation of co-culture organoids from various human iPSC clones. a, Images of organoids cultured in the absence (organoid alone, n = 9) or presence (co-culture organoid, n = 9) of iMac for 18 days. Scale bar, 500 µm. **b**, Organoid size was measured over time in the absence and presence of iMac. Statistical analysis, 2-way ANOVA (n = 9 for each condition, KYOU-1 iPSC clone). **c**, Evolution of the size of organoids generated from the XCL-1 iPSC clone over time from day 0 to day 20 in the absence and presence of iMac. Statistical analysis, 2-way ANOVA (n = 3 for each condition, representative of at least 2 separate experiments). **d**, Size of brain organoids generated from iPSC clones HD33i and IMR90 devoid of innate microglia in the presence or absence of autologous iMac from day 0 to day 16, (n = 12 each condition for each iPSC line). Statistical analysis, 2-way ANOVA. *Boxed*, proportion (%) of "innate" microglia in each organoid at day 16 (n = 8, n = 12 respectively). **e**, Size of brain organoids generated from iPSC clones CTRL, CAU, pCi-ASI and XCL-1 from day 0 and up to day 15 (day 20 for XCL-1 iPSC clone) (n = 14, 17, 11 and 9 respectively). *Boxed plots* represent the proportion (%) of innate microglia in each organoid at day 16, and the change of sizes between organoids with and without innate microglia (number of each organoid displayed on the graph). Statistical analysis, 2-way ANOVA. **f**, Impact of the presence of M-CSF in the culture medium on the proportion of innate microglia in brain organoids generated from CTRL, CAU and pCi-ASI iPSC clones (n = 8, 6 and 8 respectively). Statistical analysis, Mann Whitney test. **g**, Impact of the presence (n = 3) and absence (n = 3) of M-CSF in the organoid culture medium on the size of organoids from CTRL and CAU iPSC clones grown for up to15 days. Statistical analysis, 2-way ANOVA. **h**, Evolution of the size of organoids generated from the iPSC of 4 distinct patients (pediatric brain cancer) over 15 days with and without iMac (n = 3 for each condition). Statistical analysis, 2-way ANOVA. Statistical analysis reported on the plot are between organoids and co-culture organoids for each day under the "*ashed*" bracket. **i**, Proportion of four different cell types identified in organoids cultured in the absence (organoid alone 1, 2 and 3) or presence of iMicro (co-culture 1, 2 and 3) for 18 days. Relative cell proportions were calculated from the single cell RNA-seq data. **j**, Bar graphs showing the relative proportion of each cell type in organoids alone (n = 3) and co-cultured organoids (n = 3). The relative proportions were calculated from the single-cell RNA-seq data. Statistical analysis, Mann Whitney test. **k**, 3D encasing of TUJ1 (TUBB3) signal by $IBA1^+$ iMicro in co-culture organoid (day 16) Scale bar, 10 µm. *Right panels* represent four different angles. Scale bar, 5 µm. (one representation of multiple similar observations). **l**, Mass-spectrometry analysis of TUJ1 protein describing the presence of TUJ1 protein in day 18 iMac, iMicro, co-NPC and co-neuron. Statistical analysis, *top plot*: one-way ANOVA; *bottom plot*: Mann-Whitney test. Three independent samples (2 co-cultured organoids and 2 organoids) from the same experiment were sorted for proteomic analysis and each sample was run in triplicate. **b-f**, **j**, **l**. Error bars: mean +/− s.e.m.

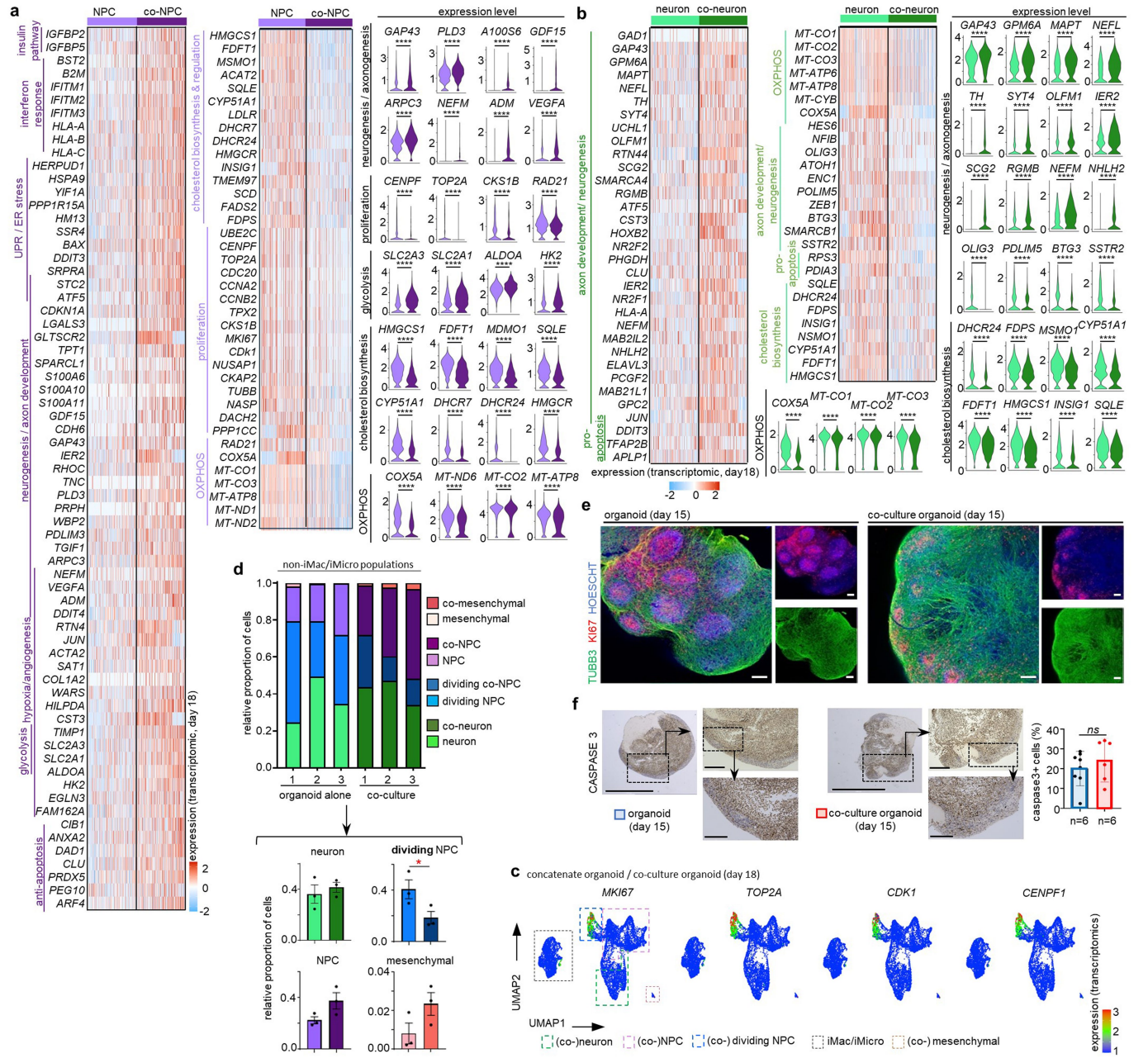

Extended Data Fig. 6 | Characteristics of NPC, co-NPC, neurons and co-neurons. a, Heatmap and associated violin plots showing the expression level of genes highly expressed in NPC or co-NPC and related pathways. **b**, Heatmap and associated violin plots showing the expression level of genes highly expressed in neuron or co-neuron and related pathways. **a, b**, *Right panels*, violin plot representation of the levels of expressions of specific genes. **c**, UMAP plots showing the expression level of canonical markers used to define proliferating cells and characterizing NPC/co-NPC in concatenated clustering analysis of organoid and co-culture organoids. **d**, Proportion of four different cell types (excluding iMicro/iMac) in organoids cultured in the absence (organoid alone 1, 2 and 3) or presence of iMac (co-culture 1, 2 and 3) for 18 days. Relative proportions of each cell types were calculated from the single cell RNA-seq data. Statistical analysis, Mann Whitney test. **a-d**, Data displayed correspond to data analysis from RNA-seq performed on cells obtained from organoid and co-culture organoid at day 18. **e**, Z-projections of immunofluorescence staining of day 15 organoids and co-culture organoids for TUBB3 (TUJ1), Ki67 and Hescht. (n = 3 and n = 2 respectively). **f**, Immunohistochemistry of brain organoid alone (n = 6) and co-culture (n = 6) for CASPASE3. Quantification analysis using QuPath software. *Boxed areas* are displayed on the right and below each pictures respectively. Scale bar, 1250 µm, 275 µm and 150 µm. Statistical analysis, Mann-Whitney U test. Error bars, mean +/− s.e.m.

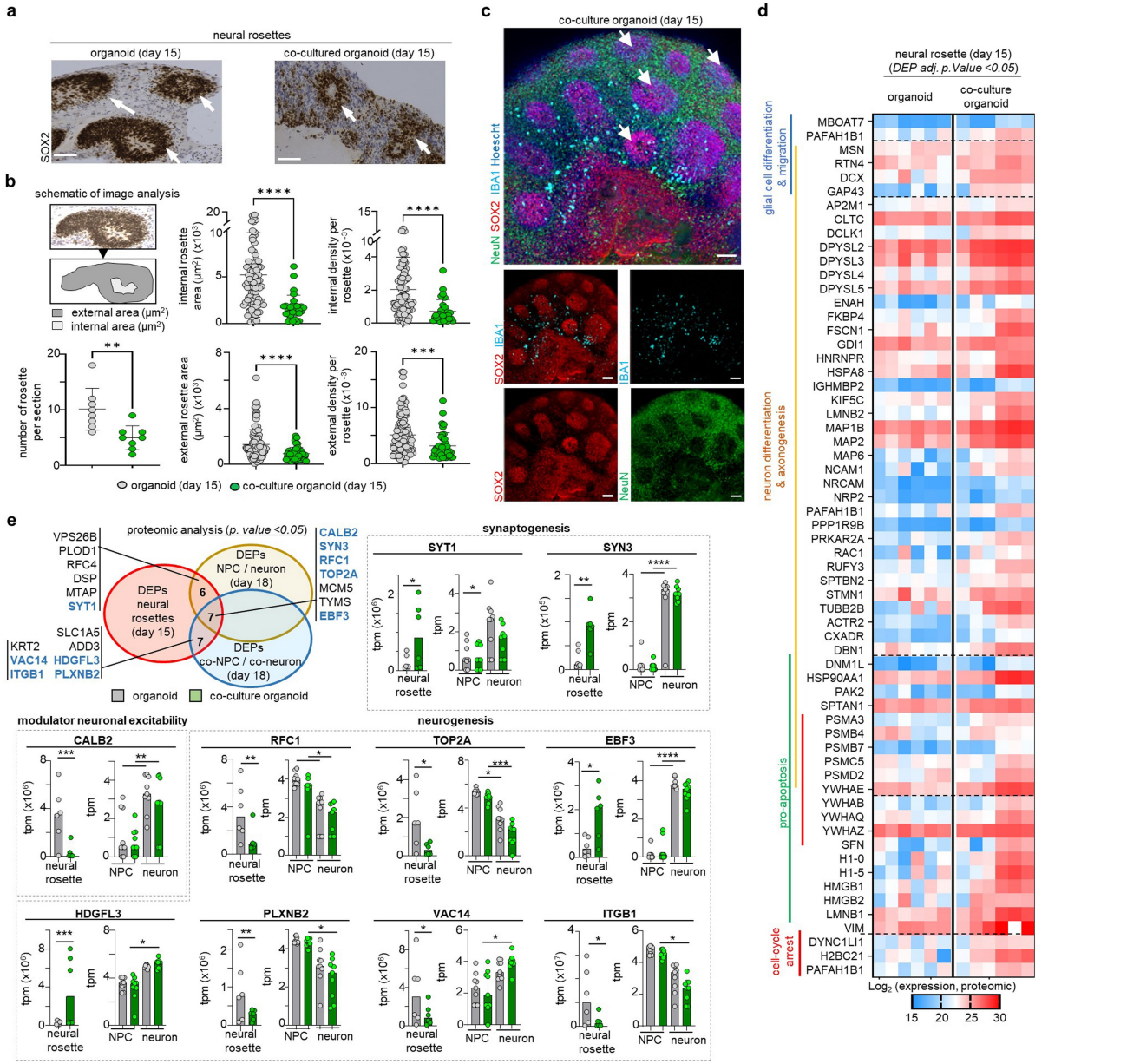

Extended Data Fig. 7 | Description of neural rosettes in co-culture organoids. a, Immunochemistry staining for SOX2 of neural rosettes from organoids (representative of 115 rosettes from 11 organoids) and co-culture organoids (representative of 40 rosettes from 8 organoids) at day 15. Scale bar, 100 µm. **b**, Description of the intrinsic features of neural rosettes from day 15 organoids and co-culture organoids. Number of rosettes per organoid section (n = 8 for each organoid culture). Representation of the internal and external rosette areas (µm²) (and associated internal and external density per rosette) for each measured rosette from organoids (n = 115) and co-culture organoids (n = 40). Statistical analysis, Mann-Whitney test. **c**. Z-stacks and associated projection showing the repartitions of IBA1⁺ iMicro, SOX2⁺ neural rosettes and NeuN⁺ neurons. Picture representative of 5 different co-culture organoids (day 15). White arrows, neural rosettes. Scale bar, 100 µm. **d**. Heatmap of DEPs from mass-spectrometry proteomic analysis of rosettes from day 15 organoids and co-culture organoids (n = 6 each, 40–50 rosettes per replicate). **e**, Expression of major proteins common between day 15 neural rosettes; and NPC, neuron, co-NPC and co-neurons (2 independent samples, 3 replicates each). Statistical analysis, Mann-Whitney test and one-way ANOVA respectively. **a, e**, Error bars, mean +/− s.e.m.

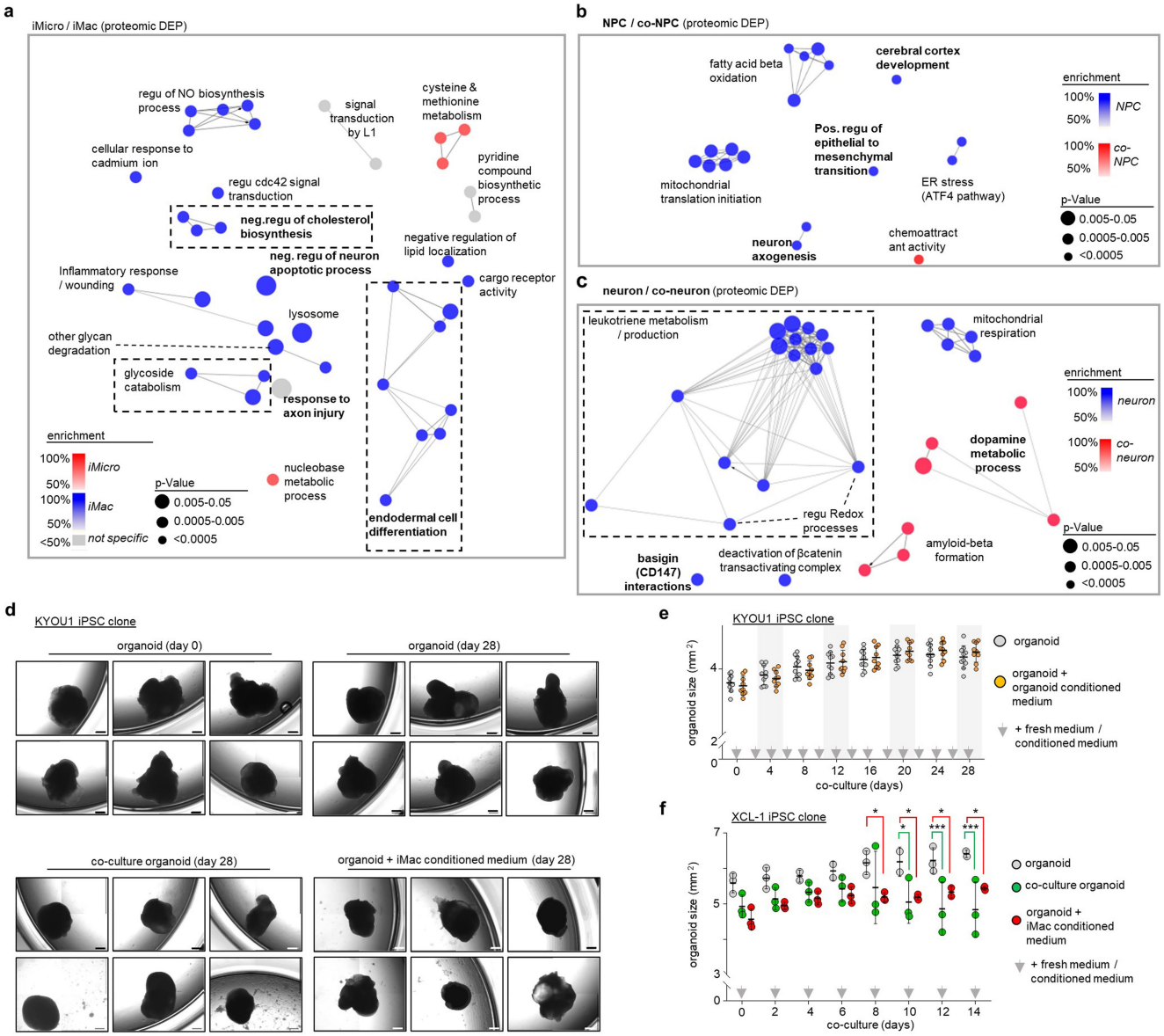

Extended Data Fig. 8 | Pathway analysis from proteomic data, impact of conditioned medium on organoid growth. a, b, c, Pathway network analysis highlighting the enrichment/loss of pathways using differentially expressed proteins (DEP) from proteomic data in iMac *versus* iMicro, NPC *versus* co-NPC and neuron *versus* co-neuron, respectively; and showing an increased neurogenesis upon the addition of iMicro. Enrichment is coded with a colour gradient. Prevalence of the pathway is reflected by its p-Value (only pathway with p-Value < 0.05 are represented). **d**, Images of organoids cultured in the absence (organoid day 0 and day 28) or presence (co-culture organoid) of iMac, or under supernatant transfer from iMac culture for 28 days. Scale bar, 500 µm. n = 6 for each condition. **e**, Change in the size of brain organoids grown in medium replaced with fresh organoid medium (n = 9) or fresh organoid conditioned medium (n = 9) every 3 days (grey arrows). Statistical analysis, 2-way ANOVA. **f**, Changes in organoid size generated from XCL-1 iPSC clone over-time in the absence and presence of iMac conditioned medium replaced every 2 days (grey arrows). Co-culture organoids were used as control. Statistical analysis, 2-way ANOVA. (n = 3 per conditions, representative of at least 2 independent experiments). **e, f**, Error bars, mean +/− s.d. regu. Regulation, pos. positive, neg. negative.

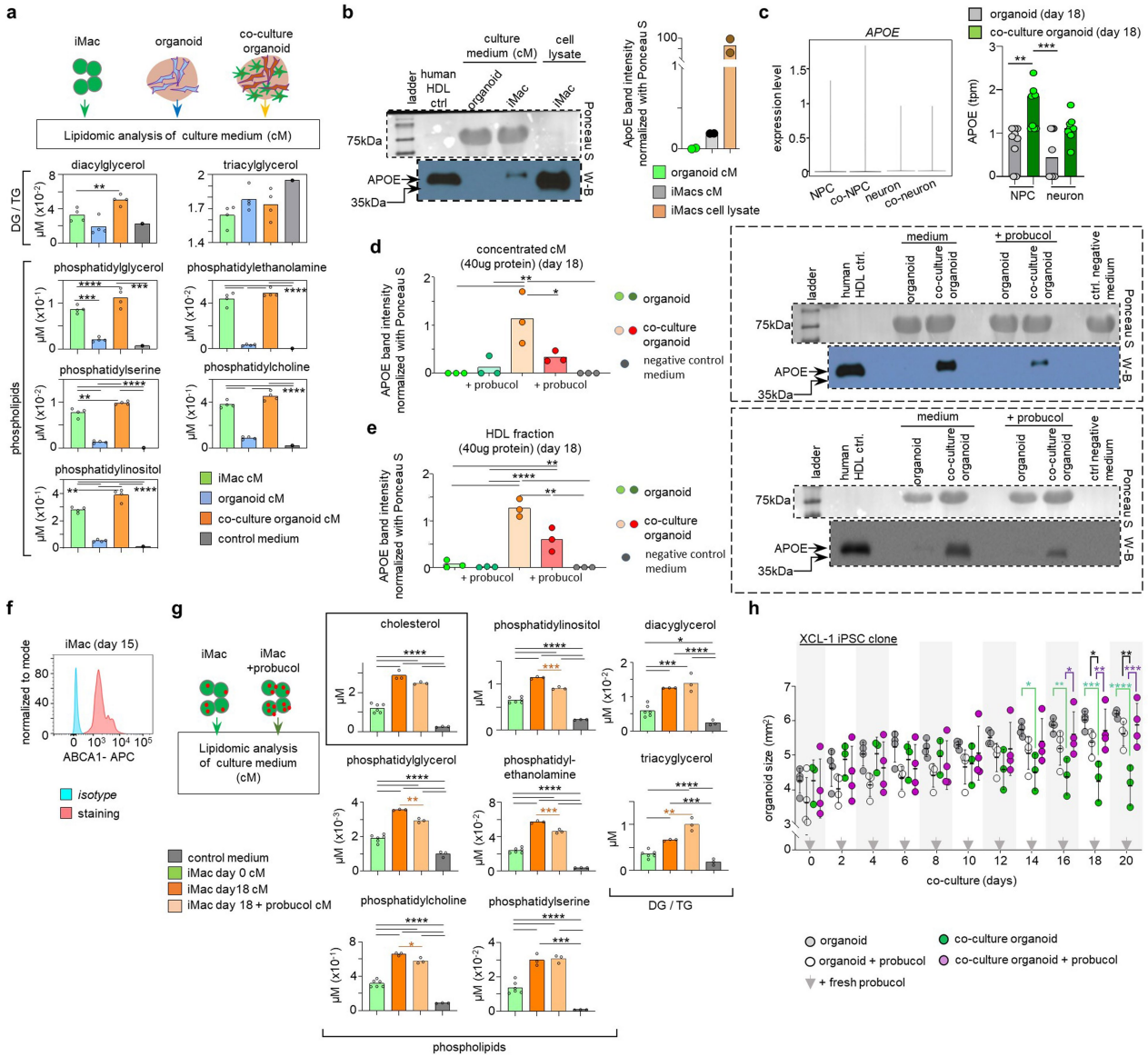

Extended Data Fig. 9 | Composition of co-culture organoid conditioned medium. a, Mass-spectrometry lipidomic analysis of culture medium (cM) from iMac, organoid and co-culture organoids at day 18. (n = 4 for cell samples, n = 1 for medium). Statistical analysis, one-way ANOVA. **b**, Western blot (W-B) analysis of iMac cell lysates and conditioned medium (cM) from iMac and organoid culture (n = 2 each). Quantitation of APOE is normalised to ponceau S signals representing 40 µg of protein loaded on the gel. Positive control: human HDL. Individual gels are shown in Supplementary Fig. 1a. **c**, Expression profile of *APOE* transcripts and APOE proteins in NPC, co-NPC, neurons and co-neurons (*left* and *right* panels respectively). Transcript, RNA-seq data from day 18 organoids. Protein, mass-spectrometry proteomic analysis on sorted cells from day 18 organoids (Three independent samples (3 co-cultured organoids and 3 organoids) sorted for proteomic analysis and each sample was run in triplicate). Statistical analysis, one-way ANOVA. **d, e**, Western blot (W-B) analysis for the expression of APOE from concentrated and HDL fraction (respectively) of day 18 organoids and co-culture organoids conditioned medium (cM) in the presence or absence of probucol. Human HDL and HDL negative medium are used as negative and positive controls respectively. HDL fractions isolated from density gradient centrifugation of cM and plasma (HDL ctrl). Quantification normalised with the protein amount loaded (40 µg). Gels are representative of 3 independent experiments. Statistical analysis, one-way ANOVA. Individual gels are shown in Supplementary Fig. 1c and d respectively. **f**, Expression profile of ABCA1 protein by flow cytometry analysis on iMac (day 18). Representative of n = 3. **g**, Mass-spectrometry lipidomic analysis of culture medium (cM) from iMac with or without treatment with probucol. n = 6 (iMac day 0), n = 3 (control medium, iMac day 18 and iMac day 18 + probucol). Statistical analysis, one-way ANOVA. **h**, Impact of probucol (added every 2 days, grey arrows) on the size of organoid and co-culture organoids from XCL-1 iPSC clone over time (up to 20 days). Untreated organoids were used as control. Statistical analysis, 2-way ANOVA. (Representative of 2 independent experiments with n = 4 each). **a, c, d, e, g**, Bar represents the mean. **h**, Error bars: mean +/− s.d). ctrl., control.

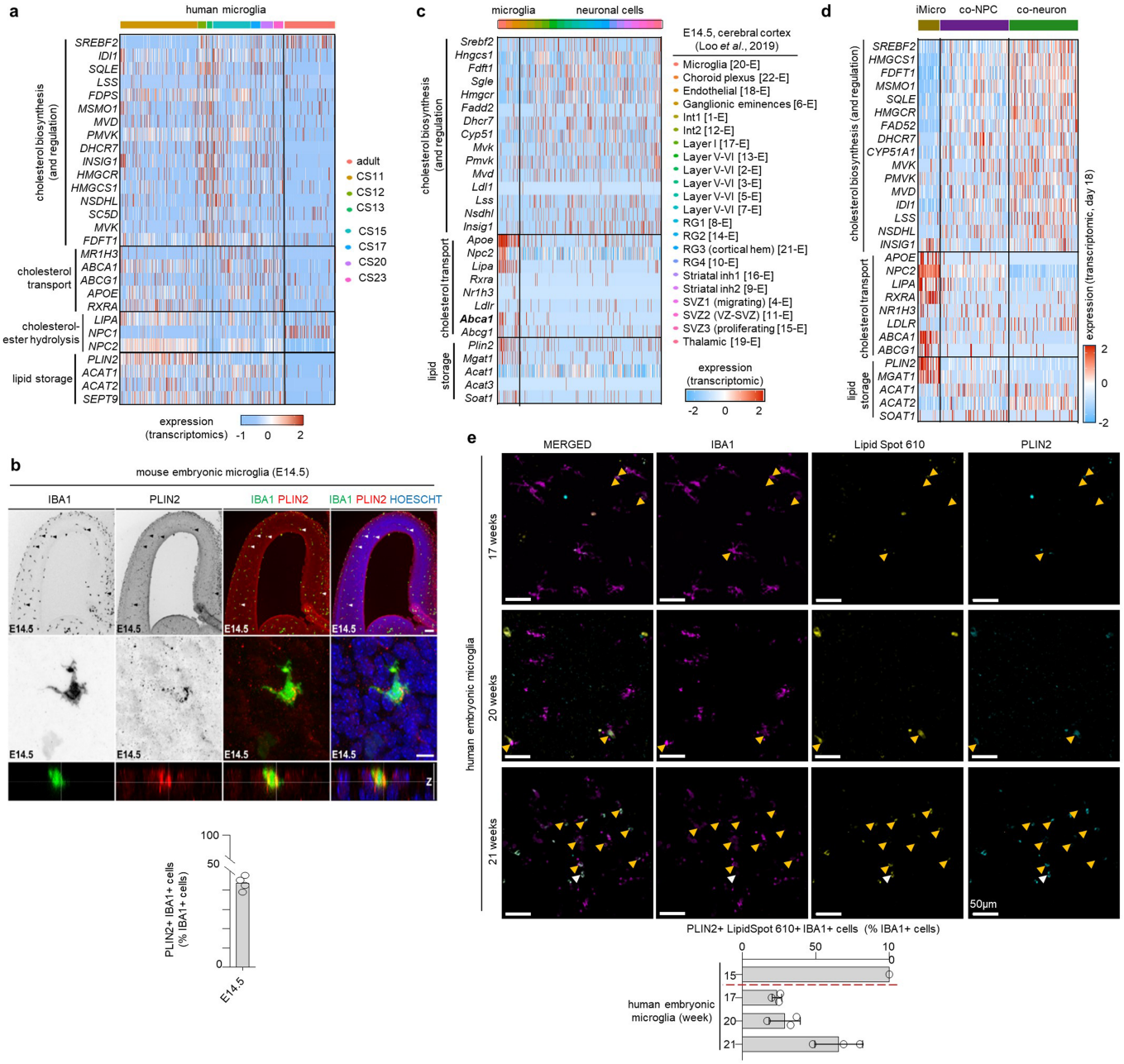

Extended Data Fig. 10 | Identification of iMicro signature in datasets and during fetal development. a, Heatmaps showing transcripts involved in cholesterol biosynthesis and regulation, cholesterol transport and lipid storage in human microglial cells at the embryonic development and adulthood stages. **b**, Immunofluorescence staining of the neocortex region of E14.5 brain for IBA1, PLIN2 and Hoechst. Analysis and quantification using the Imaris Imaging software. Picture representative of n = 4. **c, d**, Heatmaps showing transcripts involved in cholesterol biosynthesis and regulation, cholesterol transport and lipid storage in microarray data of E14.5 cerebral cortex (microglia and neuron; *Loo et al., 2019*) and in our organoid model (iMicro, co-NPC and co-neuron) respectively. **e**, Immunofluorescence staining of human foetal microglia (17, 20 and 21 weeks, n = 3 each) for Lipid-spot 610, PLIN2 and IBA1. Different magnifications are used on the samples. Scale bar, 50 µm. *Yellow arrows* characterize Lipid-spot 610$^+$ PLIN2$^+$ IBA1$^+$ cells. Picture representative of 3 independent staining from one foetal brain at week 17, 20 and 21. Quantification using the Imaris Imaging software.

nature portfolio

Corresponding author(s): Florent Ginhoux
2021-03-04531D

Last updated by author(s): 21/08/2023

Reporting Summary

Nature Portfolio wishes to improve the reproducibility of the work that we publish. This form provides structure for consistency and transparency in reporting. For further information on Nature Portfolio policies, see our Editorial Policies and the Editorial Policy Checklist.

Statistics

For all statistical analyses, confirm that the following items are present in the figure legend, table legend, main text, or Methods section.

n/a	Confirmed
☐	☒ The exact sample size (*n*) for each experimental group/condition, given as a discrete number and unit of measurement
☐	☒ A statement on whether measurements were taken from distinct samples or whether the same sample was measured repeatedly
☐	☒ The statistical test(s) used AND whether they are one- or two-sided *Only common tests should be described solely by name; describe more complex techniques in the Methods section.*
☒	☐ A description of all covariates tested
☐	☒ A description of any assumptions or corrections, such as tests of normality and adjustment for multiple comparisons
☐	☒ A full description of the statistical parameters including central tendency (e.g. means) or other basic estimates (e.g. regression coefficient) AND variation (e.g. standard deviation) or associated estimates of uncertainty (e.g. confidence intervals)
☒	☐ For null hypothesis testing, the test statistic (e.g. *F*, *t*, *r*) with confidence intervals, effect sizes, degrees of freedom and *P* value noted *Give P values as exact values whenever suitable.*
☒	☐ For Bayesian analysis, information on the choice of priors and Markov chain Monte Carlo settings
☒	☐ For hierarchical and complex designs, identification of the appropriate level for tests and full reporting of outcomes
☒	☐ Estimates of effect sizes (e.g. Cohen's *d*, Pearson's *r*), indicating how they were calculated

Our web collection on statistics for biologists contains articles on many of the points above.

Software and code

Policy information about availability of computer code

Data collection

>>No new software nor code were used for data collection
Lipidomic data were acquired by mass spectrometry using Agilent MassHunter Acquisition software (Version B.08.00, https://www.agilent.com/en/product/software-informatics/mass-spectrometry-software)
EVOS M7000 Imaging system (https://www.thermofisher.com/order/catalog/product/AMF7000?SID=srch-srp-AMF7000)
Responses of neurons are recorded at a holding potential of –70mV with the MultiClamp 700B amplifier, Axon Digidata 1550B acquisition system and Clampfit 11.1 (Molecular Devices).

Data analysis

>>No new software nor code were used to analyse data
Transcritomic Analysis: The cell ranger pipeline (version 2.1.1) was used to pre-process the 10X sequencing data generated by the 10X Genomics Chromium Controller. Illumina BCL files were converted to FASTQ files using the cellranger "mkfastq" command. Each read from the FASTQ files were then aligned to a human reference genome (GRCh38-1.2.0) using the "Cellranger count " command in order to generate count matrix.
Using Seurat R package v3.2.2 (https://satijalab.org/seurat/), the data matrices were turned into Seurat object format, combined, log-normalised, and then passed through the FindIntegrationAnchors function in Seurat in order to identify the set of anchors (Anchorset) between the two datasets. The AnchorSet was then used to integrate the datasets using the IntegrateData function.
dentity score of iMicro transcriptome compared to microglia transcriptome from the Allen Brain Atlas was done by scoring genes as per the AddModuleScore function in Seurat . Single-cell transcriptomic data were also used to construct global gene regulatory networks (regulons) using the single-cell regulatory network inference and clustering (SCENIC) R package (Version 1.1.2, https://scenic.aertslab.org/).
Pathway Analysis: The pathways network to unravel biological and metabolic functions of cells using differentially-expressed proteins (DEP) was established using ClueGO (Version 2.5.7), a plug-in application in Cytoscape (Version 1689 3.8.0). (Available at https://

cytoscape.org/)
Gene Ontology: Analysis performed using the PANTHER classification system for GO analysis according to the developers' instructions (http://www.pantherdb.org)
Proteomic Data: Data were analysed using EdgeR (Version 4.2, https://bioconductor.org/packages/release/bioc/html/edgeR.html) in RStudio (Version 4.1.2, https://www.rstudio.com/).Identification was performed using Proteome Discoverer (Version 2.5) associated with Mascot algorithm (Version 2.5). Validation of identification and quantification was performed using Software Proline Web 2.1.
Lipidomic analysis: Lipidomic data acquired by mass spectrometry were analyzed using Agilent MassHunter Quant software (Version B.08.00, https://www.agilent.com/en/product/software-informatics/mass-spectrometry-software/data-analysis/quantitative-analysis).
Electrophysiology: Data were analyzed using AxoGraph Ver 1.7.0 (AxoGraph Company, https://axograph.com/)
Western Blot: Band intensity were quantified by imageJ (free software download: https://imagej.en.softonic.com/?ex=DINS-635.2).
Microscopy analysis: Data were analysed using the Imaris (Version 9.7.0, https://imaris.oxinst.com/) and ImageJ (Version 2.9.0, https://imagej.nih.gov/ij/) softwares.
Data are represented using Graphpad Prism 9 (Version 9.5.1 (733), subscription software, https://www.graphpad.com/)

For manuscripts utilizing custom algorithms or software that are central to the research but not yet described in published literature, software must be made available to editors and reviewers. We strongly encourage code deposition in a community repository (e.g. GitHub). See the Nature Portfolio guidelines for submitting code & software for further information.

Data

Policy information about availability of data

All manuscripts must include a data availability statement. This statement should provide the following information, where applicable:

- Accession codes, unique identifiers, or web links for publicly available datasets
- A description of any restrictions on data availability
- For clinical datasets or third party data, please ensure that the statement adheres to our policy

Data availability statement is provided in the manuscript. Data have been uploaded as follow: The raw RNA-seq and bulk-seq sequencing data of this study have been deposited in Gene Expression Ominbus with accession no. GSE241127 and (Data uploaded; Pending attribution of accession number) respectively. Proteomic data on purified cell populations have been deposited on JPOST (JPST001822) and Proteome Exchange (PXD042344). Neural rosette proteomic data are available via ProteomeXchange with identifier PXD044406. All lipidomic data have been deposited in Metabolights with accession number (Data uploaded; Pending attribution of accession number)

Research involving human participants, their data, or biological material

Policy information about studies with human participants or human data. See also policy information about sex, gender (identity/presentation), and sexual orientation and race, ethnicity and racism.

Reporting on sex and gender	Our patient-derived iPSCs were generated from 3 boys (patient 515, 519 and 534) and 1 girl (patient 523) with H3K27M diffuse midline glioma. This information has been collected from the anonymized case report form (CRF) filled by the patient's medical doctor after having obtained patient/family's consent. No sex-based analysis was performed for the purpose of this paper due to the low number of patients.
Reporting on race, ethnicity, or other socially relevant groupings	No data on socially constructed or socially relevant categorization variable(s) was collected for these patients.
Population characteristics	Our patient-derived iPSCs were generated from pediatric patients with H3K27M diffuse midline glioma. They had a skin biopsy at diagnosis which was used to generated iPSC from fibroblasts for the purpose of this research. They received local radiotherapy and targeted treatment selected based on the biopsy results.
Recruitment	Four consecutive pediatric patients with a H3K27M diffuse midline glioma for whom we could obtain a fibroblast culture were included in the study.
Ethics oversight	Gustave Roussy Ethic Committee

Note that full information on the approval of the study protocol must also be provided in the manuscript.

Field-specific reporting

Please select the one below that is the best fit for your research. If you are not sure, read the appropriate sections before making your selection.

☒ Life sciences ☐ Behavioural & social sciences ☐ Ecological, evolutionary & environmental sciences

For a reference copy of the document with all sections, see nature.com/documents/nr-reporting-summary-flat.pdf

Life sciences study design

All studies must disclose on these points even when the disclosure is negative.

Sample size	No methods were used to predetermine sample sizes. Minimum sample sizes were determined based on previously published studies. At

Sample size	least 3 independently generated samples were used for data collection. The sample numbers used for analysis is specified in the figure legends. Information is reported in the manuscript where appropriate
Data exclusions	No Data were excluded
Replication	Findings were confirmed with replicate experiments as noted in the figure legends and methodology where appropriate Multiple iPSC cell lines were used to confirm the organoid size reduction after co-culture with iMacs, this is extensively described throughout the manuscript
Randomization	Brain organoids were randomly assigned for co-culture with iMacs
Blinding	Image analysis was automated and blinded such as the measurement of neurite numbers and lengths; or electrophysiological measurements. Where appropriate, control and co-cultured groups were routinely processed in parallel using the same experimental conditions to reduce bias

Reporting for specific materials, systems and methods

We require information from authors about some types of materials, experimental systems and methods used in many studies. Here, indicate whether each material, system or method listed is relevant to your study. If you are not sure if a list item applies to your research, read the appropriate section before selecting a response.

Materials & experimental systems

n/a	Involved in the study
☐	☒ Antibodies
☐	☒ Eukaryotic cell lines
☒	☐ Palaeontology and archaeology
☐	☒ Animals and other organisms
☒	☐ Clinical data
☒	☐ Dual use research of concern
☒	☐ Plants

Methods

n/a	Involved in the study
☒	☐ ChIP-seq
☐	☒ Flow cytometry
☒	☐ MRI-based neuroimaging

Antibodies

Antibodies used

Rabbit anti-Iba1 WakoCat # 019-19741
Chicken anti-Iba1 Synaptic System Cat# 234009
Goat anti-Iba1 Abcam Cat# ab5076
Mouse anti-ABCA1 Abcam Cat# ab18180
Goat anti-Sox2 RnD Cat # AF2018
Rabbit anti-Sox2 Abcam Cat # AB97959
Mouse anti-Tuj1 AbcamCat # AB78078
Mouse anti-Tuj1 Promega Cat # G712A
Mouse anti-Nestin MerckCat # MAB5326
Mouse anti-Ki67 BiolegendCat # 350514
Mouse anti-Ki67 DAKO Cat # M7240
Rabbit anti-Ki67 Abcam Cat # AB15580
Mouse anti-Plin2 ProteintechCat # ABIN1724917
Rabbit anti-Plin2 Antibodies-onlineCat # 15294-1-AP
Mouse anti-CD45 BiolegendCat # 368516
Mouse anti-CD14 BiolegendCat # 325604; 301834
Mouse anti-CD11b BD BiosciencesCat # 557918
Mouse anti-CD11b eBioscience Cat # 25-0118-42
Mouse anti-CD163 BD BiosciencesCat # 562670
Mouse anti-CXCR4 BiolegendCat # 306516
Mouse anti-CD44 BiolegendCat # 338806
Mouse anti-CD271 BD BiosciencesCat # 743358
Mouse anti-CD24 BD BiosciencesCat # 561646
Mouse anti-CD15 BiolegendCat # 323034
Mouse anti-P2RY12 BiolegendCat # 392104
Rat anti-CX3CR1 BiolegendCat # 341626; 341608
Rabbit anti-Tmem119 Sigma-AldrichCat # HPA051870-100UL
Mouse anti-CD80 BD Pharmingen Cat# 557227
Mouse anti-CD86 BD Pharmingen Cat# 555665
Mouse anti-CD68 Biolegend Cat# 333808
Mouse anti-HLA-DR Biolegend Cat# 327014
Mouse anti-b3tubulin PromegaCat # G712A
Mouse anti-NeuN SigmaCat # MAB377
Alexa-Fluor 488-conjugated donkey anti-mouse Jackson ImmunoResearch Cat# 715545150
Cy3-conjugated donkey anti-rabbit Jackson ImmunoResearch Cat# 711165152
Cy5-conjugated donkey anti-chicken Jackson ImmunoResearch Cat# 703175155

	Donkey anti-Goat IgG (H+L) Cross-Adsorbed Secondary Antibody, Alexa Fluor™ 488 Invitrogen Cat # A-11055 APC Conjugation Kit (LNK03)- BioRad Cat# LNK032APC
Validation	The majority of antibodies used in this study were selected from published literature or which use has been optimized accordingly in the lab or by collaborators. Where possible they were validated and optimized using human primary cells as well as titration to ensure the optimal final concentration and cell number.

Eukaryotic cell lines

Policy information about cell lines and Sex and Gender in Research

Cell line source(s)	Human iPSC KYOU1 (KYOU-DXR0109B, 1217 #ACS-1023) and IMR-90 (#CCL-186) were obtained from ATCC. CTRL iPSC line was obtained from Dr Ragnhildur Thora Karadottir. CAU iPSC was obtained from Atlantis Bioscience (#PCi-KER_KIT), HD33i from the NINDS iPSC Repository at Coriell Institute (#ND36997), PCi-ASI from Phenocell (#PCi-ASI_0.5M) and XCL-1 from XCell Science (#IP-001-1V).
Authentication	IPSC lines were confirmed by fluorescence / IF staining, RNAseq, and karyotyping.
Mycoplasma contamination	All cell Lines were routinely tested and found negative for mycoplasma
Commonly misidentified lines (See ICLAC register)	No misidentified lines were used int he study

Animals and other research organisms

Policy information about studies involving animals; ARRIVE guidelines recommended for reporting animal research, and Sex and Gender in Research

Laboratory animals	C57BL/6J mice were sacrificed at E13.5, E14.5, P0 and 15 weeks old, and the brains were harvested and imaged.
Wild animals	No wild animals were used in this study
Reporting on sex	N/A
Field-collected samples	No field-collected samples were used in this study
Ethics oversight	C57BL/6 mice (CD45.1 and CD45.2) were from the Biological Resource Center, Agency for Science, Technology and Research, Singapore. All experiments and procedures were approved by the Institutional Animal Care and Use Committee of the Biological Resource Center (Agency for Science, Technology and Research, Singapore) in accordance with the guidelines of the Agri-Food and Veterinary Authority and the National Advisory Committee for Laboratory Animal Research of Singapore (ICUAC No. 151071).

Note that full information on the approval of the study protocol must also be provided in the manuscript.

Flow Cytometry

Plots

Confirm that:

☒ The axis labels state the marker and fluorochrome used (e.g. CD4-FITC).

☒ The axis scales are clearly visible. Include numbers along axes only for bottom left plot of group (a 'group' is an analysis of identical markers).

☒ All plots are contour plots with outliers or pseudocolor plots.

☒ A numerical value for number of cells or percentage (with statistics) is provided.

Methodology

Sample preparation	Brain organoids were washed 5 times in PBS and incubated in digestion buffer containing Stempro Accutase, Collagenase (Merck, 1480 C5138) and DNase (Merck, #10104159001) for 30 minutes at 37°C. The organoids were then gently pipetted up and down 10 times using a 1ml pipette tip in order to release the cells from the organoids. Remaining cells were released from organoids by agitation at 1,400 rpm on an Eppendorf Thermomixer C, at 37°C for 10 mins before gently pipetting up and down 10 times using a 1 ml tip. Once the cell debris had settled at the bottom of the tube, the supernatant was gently collected, and filtered through 70 µm filter paper. The cell suspension was then washed in FACS buffer, centrifuged, and the cell pellet collected. The pellet was suspended and incubated in blocking buffer (PBS containing 5% FCS) containing the specified antibodies for 30 mins at 4°C. Cells were then incubated with DAPI for nuclear staining and analysed by flow cytometry. iMacs were washed 3 times in PBS and stained as described. All sample preparatoins are extnesively described in the methodology section.
Instrument	BD FACSARIA II/III or BD LSRII (BD Bioscience)

Software	Flowjo was used to collect and analyze the data
Cell population abundance	The cells were sorted, seeded and cultured on a culture dish. Immunostaining was performed using markers to confirm the identity and purity of the cells. Cell population statistics are reported in terms of absolute number or percentage (%) as described in the figure keys.
Gating strategy	Gating strategy is shown where appropriate. Iotype controls were used to determine positivity / negativity.

☒ Tick this box to confirm that a figure exemplifying the gating strategy is provided in the Supplementary Information.